Journal of Innate Immunity

Research Article

J Innate Immun 2023;15:204–221
DOI: 10.1159/000526121

Received: November 17, 2021
Accepted: June 27, 2022
Published online: September 16, 2022

Cathelicidins Induce Toll-Interacting Protein Synthesis to Prevent Apoptosis in Colonic Epithelium

Ravi Holani[a] Chathurika Rathnayaka[a] Graham A.D. Blyth[a] Anshu Babbar[a] Priyoshi Lahiri[a] Daniel Young[b, c] Antoine Dufour[b, c] Morley D. Hollenberg[b, d] Derek M. McKay[b, d] Eduardo R. Cobo[a, d]

[a]Department of Production Animal Health, Faculty of Veterinary Medicine, University of Calgary, Calgary, AB, Canada; [b]Department of Physiology & Pharmacology, Cumming School of Medicine, University of Calgary, Calgary, AB, Canada; [c]McCaig Institute for Bone and Joint Health, Cumming School of Medicine, University of Calgary, Calgary, AB, Canada; [d]Calvin, Phoebe and Joan Snyder Institute for Chronic Disease, Cumming School of Medicine, University of Calgary, Calgary, AB, Canada

Keywords
Colonic epithelium · Apoptosis · TOLLIP · Cathelicidin · miRNA

Abstract
Cathelicidin peptides secreted by leukocytes and epithelial cells are microbicidal but also regulate pathogen sensing via toll-like receptors (TLRs) in the colon by mechanisms that are not fully understood. Herein, analyses with the attaching/effacing pathogen *Citrobacter rodentium* model of colitis in cathelicidin-deficient (*Camp*$^{-/-}$) mice, and colonic epithelia demonstrate that cathelicidins prevent apoptosis by sustaining post-transcriptional synthesis of a TLR adapter, toll-interacting protein (TOLLIP). Cathelicidins induced phosphorylation-activation of epidermal growth factor receptor (EGFR)-kinase, which phosphorylated-inactivated miRNA-activating enzyme Argonaute 2 (AGO2), thus reducing availability of the TOLLIP repressor miRNA-31. Cathelicidins promoted stability of TOLLIP protein via a proteosome-dependent pathway. This cathelicidin-induced TOLLIP upregulation prevented apoptosis in the colonic epithelium by reducing levels of caspase-3 and poly (ADP-ribose) polymerase (PARP)-1 in response to the proinflammatory cytokines, interferon-γ (IFNγ) and tumor necrosis factor-α (TNFα). Further, *Camp*$^{-/-}$ colonic epithelial cells were more susceptible to apoptosis during *C. rodentium* infection than wild-type cells. This anti-apoptotic effect of cathelicidins, maintaining epithelial TOLLIP protein in the gut, provides insight into cathelicidin's ability to regulate TLR signaling and prevent exacerbated inflammation.

Introduction

Small cationic cathelicidin peptides secreted by intestinal epithelial cells and leukocytes in response to inflammatory and bacterial stimuli [1, 2] have been repurposed as immunoregulators of inflammation and host innate defenses [3, 4], given that their microbicidal role may be

Present address: Ravi Holani, Michael Smith Laboratories, Faculty of Medicine, University of British Columbia, Kelowna, BC, Canada.

Karger@karger.com
www.karger.com/jin

Correspondence to:
Eduardo R. Cobo, ecobo@ucalgary.ca

restricted during in vivo settings [3, 5]. The antibacterial effect of cathelicidins is limited in the presence of sugars [6], high salt content [7], and modified bacterial surfaces (e.g., acetylated *Salmonella* lipopolysaccharide [LPS], derived lipid A) [8]. Moreover, in vitro demonstration of microbicidal activity typically requires concentrations of cathelicidins >10 mM, which are cytotoxic to mammalian cells [9, 10] and far exceed reported physiological concentrations (0.5–6 μM) achieved by the single form of human cathelicidin, leucine-leucine with 37 amino acid residues (LL-37) encoded by the *cathelicidin antimicrobial peptid*e (*CAMP*) gene [11].

At low non-antimicrobial concentrations (i.e., <2–4 μM) [12], cathelicidins can be internalized and modulate the function of mast cells, leukocytes, and epithelial cells [4]. For instance, LL-37 promotes mast cell degranulation [13], neutrophil and macrophage chemotaxis [14–16], and macrophage phagocytosis by interacting with integrin αMβ2 (Mac-1) [17], Fcγ receptors, formyl peptide receptor (FPR) 2 [18], or the purinergic P2X7 receptor [19, 20]. A putative critical role of cathelicidins is the detection of damage- and microbe-associated molecular patterns and regulation of toll-like receptor (TLR) responses [3–5, 21–24]. Regulation of TLRs by cathelicidins has been attributed to their binding to TLR ligands (e.g., LPS: [25, 26]) and direct modulation of TLR signaling [4, 21]. For example, LL-37 prevents LPS-evoked tumor necrosis factor-α (TNFα) secretion from macrophages by inhibiting the nuclear factor kappa-light-chain-enhancer of activated B cells (NF-kβ) pathway [21] and evokes CXCL8 secretion in LPS-stimulated colonic epithelial cells by facilitating intracellular LPS-TLR4 endosomic signaling [27]. Moreover, low doses of LL-37 enhance expression and cytoplasmic translocation of TLR-4 in mast cells via EGFR and FPR2 [28]. Other TLR regulatory functions of LL-37 include reduction of monocyte chemoattractant protein-1 (MCP-1) synthesis in human periodontal ligament cells after LPS challenge [29] and downregulated expression of the proinflammatory triggering receptor expressed on myeloid cell (TREM-1) in peripheral blood mononuclear cells stimulated by TLR2 and TLR4 ligands [30]. Non-mammalian cathelicidins from *Alligator sinensis* [31] and green sea turtle [32] likewise prevent LPS binding to TLR4, reducing nitric oxide, and TNF-α, IL-1β and IL-6 production in murine macrophages. Specific LL-37 amino acid sequences enable intracellular immune recognition of endogenous/self-nucleic acids, RNA [33], and DNA [34]. The murine homologue of cathelicidin, cathelicidin-related antimicrobial peptide (CRAMP) encoded by the *Camp* gene [35], has been also shown to regulate cellular responses to TLR ligands. Bone marrow-derived macrophages from CRAMP-deficient mice ($Camp^{-/-}$) challenged by LPS secrete more IL-10 compared to wild-type counterparts [36]. Regarding cell lifespan, LL-37 prevents apoptosis in primary human keratinocytes exposed to camptothecin, a chemotherapeutic DNA topoisomerase l inhibitor [37]. Likewise, pretreatment of mice with a cathelicidin peptide isolated from the snake *Bungarus fasciatus* prevents LPS-induced apoptosis in jejunal epithelium [38].

Despite repeated demonstration of cathelicidin modulation of TLR-driven events, the underlying mechanisms remain elusive. Of particular interest is the intracellular TLR adapter toll-interacting protein (TOLLIP) [39]. TOLLIP blocks NF-kβ activation after IL1R, TLR2, and TLR4 activation by interacting with the toll/interleukin-1 receptor (TIR) domain of the IL1 receptor (IL1R) and by inhibiting phosphorylation-dissociation of N-terminus of the IL1 receptor-associated kinase 1 (IRAK-1) [39–41]. Ubiquitously expressed in many tissues [39] including the colon [42, 43], TOLLIP is critical in colitis; $Tollip^{-/-}$ mice are highly susceptible to dextran sodium sulfate (DSS)-induced colitis [40, 42] and colitis-associated cancer [43]. Direct effects of cathelicidin on TOLLIP and mechanism of action in colon homeostasis are largely unknown. It has been reported that a low dose of LL-37 in combination with *Porphyromonas gingivalis*-derived LPS reduces TLR4 and CD14 gene expression and enhances transcriptional expression of TLR adapters including TOLLIP in human-derived gingival fibroblasts [44]. In the current study, we reveal that cathelicidins sustained TOLLIP expression in colonic epithelial cells, via post-transcriptional prevention of miRNA-degradation. Such cathelicidin-induced regulation of a TLR adapter molecule key in NF-kβ regulation enhanced epithelial cell survival in vitro and during *Citrobacter rodentium*-evoked colitis.

Materials and Methods

Colonic Epithelium and Fibroblast Culture

Human colon adenocarcinoma-derived HT29 epithelial cells and murine subcutaneous connective tissue-derived L929 fibroblasts (provided by Dr. K. Chadee, Uni. Calgary) were cultured in Dulbecco's Modified Eagle's Medium (DMEM; Gibson, Life Technologies) and Roswell Park Memorial Institute 1640 medium, respectively, supplemented with 10% fetal bovine serum (FBS; Benchmark Gemini Bio-Products), 1% penicillin (100 U mL^{-1})/streptomycin (100 μg mL^{-1}; HyClone Thermo Fisher Scientific) in a humidified environment with 5% CO_2. For experiments, cells were cultured in serum-free and antibiotic-free medium. Cellular

receptor signaling was studied using chemical inhibitors (1 h pretreatment and through the experiment) for proteosomes (MG132, HY-13259; MedChemExpress), human FPRL1 (WRW4, 2262; Tocris Bioscience), P2X7 (A740003, 3701; Tocris Bioscience), and EGFR-kinases (AG1478 hydrochloride, 1276; Tocris Bioscience) [27]. LPS from *S. typhimurium* (100 ng/mL; L6143, Sigma-Aldrich) was used as a control in L929 fibroblast experiments as this dose combined with LL-37 (2 μM) induces IL-8 in HT29 cells [27].

Murine C. rodentium *Colitis*

Experiments to induce *C. rodentium* colitis were conducted on male C57/BL6 (8-week-old, 20–25 gm weight) wild-type *Camp*$^{+/+}$ and cathelicidin-null *Camp*$^{-/-}$ mice (B6.129X1-*Camp*^{tm1Rlg}/J; The Jackson Laboratory) littermates that had been co-housed for up to 10 generations in a pathogen-free environment (Univ. Calgary) with ad libitum access to water and standard rodent chow diet. Animal research studies were performed in accordance with the Canadian Guidelines for Animal Welfare and the Univ. Calgary Animal Care Committee (AC20-0050) and reported following ARRIVE guidelines https://arriveguidelines.org/arrive-guidelines. Studies were conducted in males because sex differences have not been observed in *C. rodentium* clearance or in the severity of the infection-induced colitis in mice [45], and neutrophil activation by closely related *Escherichia coli* is similar in males and females [46]. For infective challenge, *C. rodentium* was cultured on MacConkey agar plates (16 h, 37°C), and a single colony was sub-cultured in LB broth (5 mL, 16 h, 37°C) without shaking. Littermates were orally inoculated (200 μL) with PBS or *C. rodentium* (DBS-100) at ~5 × 10^8 CFU, previously reported as effective to colonize C57/BL6 mice [47]. Mice were humanely euthanized 7 days postinfection (dpi).

In restitutive experiments, *Camp*$^{+/+}$ and *Camp*$^{-/-}$ mice challenged with *C. rodentium* were injected intraperitoneally (ip.) with synthetic CRAMP (AL0109; Shanghai Royobiotech, peptide sequence: H-Gly-Leu-Leu-Arg-Lys-Gly-Gly-Glu-Lys-Ile-Gly-Glu-Ly-Leu-Lys-Lys-Ile-Gly-Gln-Lys-Ile-Lys-Asn-Phe-Phe-Gln-Lys-Leu-Val-Pro-Gln-Pro-Glu-Gln-OH with trifluoroacetate salt, purity of >95%) at −1, 1, 3, and 5 dpi (8 mg/kg of body weight per dose). This dose was selected because injection of CRAMP (5–10 mg/kg) into intestinal loops reduced *Clostridium difficile*-induced colitis [48, 49], daily intrarectal delivery alleviated DSS model of colitis [50], and given ip. mitigated diabetic [51], hypertrophy [52] cardiomyopathies, and *Candida albicans* infection [53].

Isolation of Murine Primary Colonic Epithelial Cells

Whole colons were aseptically removed from healthy male 8-week-old wild-type *Camp*$^{+/+}$ and *Camp*$^{-/-}$ mice, rinsed with cold PBS (1X), opened longitudinally, sectioned (2-cm pieces), and suspended in isolation PBS buffer (10 mL) containing EDTA (5 mM; 15575020; Thermo Fisher Scientific) and DTT (0.324 M; D0632; Sigma-Aldrich). Isolated cells were incubated (37°C, 20 min on a rocker-shaker), passed through a cell strainer (70 μm; 10199656; VWR), washed with cold PBS (3X), and processed for protein isolation. Purity of this primary colonic epithelial cell population was determined as CD326$^+$ (563477; BD Bioscience) CD45$^-$ (103139; BD Bioscience) cells using flow cytometry (~85–90%; data not shown).

Murine Colonoids

Mini 3D-gut spheroids were developed from murine colonic crypts [54]. Whole colon was excised aseptically, cleaned to remove excess fat and mesentery, opened longitudinally, thoroughly washed with PBS, cut (<1 mm), and suspended in 5 mM EDTA-PBS solution (20 min, 4°C). Crypts were isolated by vigorous shaking, filtered (70 μm), and cultured on Matrigel matrix using IntestiCult™ Organoid Growth Media (Stem Cell Technologies) for 10 days until colonoid morphology was apparent. For experiments, colonoids suspended in Matrigel were basolaterally stimulated with synthetic LL-37 (2 μM; for up to 8 h) added to culture media and proteins isolated as described below.

Isolation of Murine Bone Marrow Macrophages

Bone marrow macrophages were isolated from femurs and tibias aseptically removed from *Camp*$^{+/+}$ and *Camp*$^{-/-}$ mice [55]. Upon isolation, bone marrow macrophages were cultured (6 days) for macrophage lineage differentiation in Roswell Park Memorial Institute 1640 medium supplemented with 10% FBS, 2 mM L-glutamine, 50 μM 2-mercaptoethanol, 10 mM HEPES buffer (pH 7.4), 1% penicillin (100 U mL^{-1})/streptomycin (100 μg mL^{-1}), and 10% conditioned media from L929 cells (as a source of macrophage colony-stimulating factor).

TOLLIP, LL-37, and MIR31 Plasmid Transfection into Colonic Epithelial Cells

A short hairpin (Sh)-TOLLIP pGFP-V-RS, (Sh)-LL-37 pGFP-V-RS, MIR31 pCMV-MIR plasmid vector, or noneffective scrambled shRNA construct (sham) (TG320555 and TG314213; Origene) was transfected into confluent HT29 cells (HT29ShTOLLIP, HT29ShLL-37, and HT29MIR31, respectively) using Cell Line Nucleofector® Kit V (VCA-1003; Lonza). Transfected cells were selected for puromycin (30 μg/mL for ShLL-37 and 5 μg/mL for ShTOLLIP) or neomycin (800 μg/mL for MIR31) resistance. Cells were maintained in DMEM supplemented with either puromycin (15 μg/mL for ShLL-37 and 2.5 μg/mL for ShTOLLIP) or neomycin (400 μg/mL for MIR31).

Apoptosis Assessment in Colonic Epithelium

HT29 cells were treated with LL-37 at various doses and/or times as indicated in the figures, followed by a treatment regime that consistently induces apoptosis composed of TNFα (10–100 ng/mL; 210-TA-005/CF; R&D) and IFNγ (300 IU/mL; 285-IF-100/CF; R&D) for 16 h. Cytokine-induced apoptosis was determined by cleavage of caspase-3 and poly (ADP-ribose) polymerase (PARP)-1 in cell lysates using Western blotting. Cell death was monitored by assessing the content of lactate dehydrogenase (LDH) in cell supernatants (Pierce™ LDH Cytotoxicity Assay, 88953; Thermo Fisher Scientific).

Protein Determination by Western Blotting

Total proteins from cell lysates were isolated using denaturation cell extraction buffer with a protease and phosphatase inhibitor cocktail. Extracted proteins were blotted using specific primary antibodies to detect human TOLLIP (ab187198; Abcam and 4748; Cell Signaling Technology), murine TOLLIP (97632; NovusBio), cleaved caspase-3 (9661; Cell Signaling Technology), cleaved PARP (9542; New England Biolabs), phospho-EGFR-Tyr1068 (2234; Cell Signaling Technology), phospho-Argonaute 2-Ser393 (ab215746; Abcam), LL-37 (NBP46781; Novus Biologicals), and human GAPDH-6C5 (1001; Calbiochem). Antibodies were diluted 1:1,000 in PBS (1×) containing 5% bovine serum albumin, unless listed otherwise for specific antibody. Horseradish-

peroxidase-conjugate goat anti-mouse IgG (H + L) (115-035-146; Jackson ImmunoResearch; 1:10,000 in PBS) or horseradish-peroxidase goat anti-rabbit IgG (H + L) (115-035-144; Jackson ImmunoResearch; 1:10,000 in PBS) were used as secondary antibodies and developed using the Clarity Western ECL Detection System (BioRad). Image capture and densitometric analyses were performed with the ChemiDoc MP Imaging system and ImageLab 4.0.1 software (BioRad), respectively. Normalization was done with reference to the Western blot signal for GAPDH (housekeeping protein). Results were reported as fold change of target expression in stimulated groups, compared to unstimulated control groups.

Gene Transcription Analysis by Quantitative Real-Time Polymerase Chain Reaction

Transcription mRNA of TOLLIP and inflammatory cytokines in human and murine colons were quantified by quantitative real-time polymerase chain reaction (qPCR). Total RNA was isolated by conventional methods (Ribozol™ RNA extraction), and for microRNA (miR)-31-5p, total RNA was subjected to poly A tailing prior to cDNA synthesis (95107; QuantaBio). miR-31-5p abundance was assessed using MystiCq® microRNA qPCR assay primer for miR-31-5p (MIRAP00090; Sigma-Aldrich) and RNU6-1 (MIRCP00001; Sigma Adrich). Expression of mRNA was quantified by qPCR using predesigned primers (RT^2 qPCR Primer Assay; Qiagen) specific for human *TOLLIP* (PPH05844C; NM_019009), human *IFN-γ* (PPH00380C; NM_000619), human *TNF-α* (PPH00341F;NM_000594),human interleukin *IL-1β* (PPH00171C; NM_000576), human *GAPDH* (PPH00150F; NM_002046.5), murine *TOLLIP* (PPM06269E; NM_023764), murine *Gapdh* (PPM02946E; NM_008084) with verified specificity and efficiency (>95%) to ensure amplification of a single product of the correct size, as indicated in MIQE guidelines [56]. Target gene mRNA values were corrected relative to the normalizer, RNU6-1 (for miRNA) or *GAPDH* (for mRNA). Data were analyzed using the $2^{-\Delta\Delta CT}$ method and reported as mean fold change of target transcript levels in stimulated groups versus untreated control groups.

Determination of Secreted Cytokines into Colonic Epithelial Cells

Secreted CXCL1, IL10, IL8 in supernatants and IL1Rα in lysates were quantified by ELISAs (DY275, DY217B, DY208, DY280 R&D Systems, respectively) in HT29 cells and reported as absolute values (picograms per milliliter).

TOLLIP Expression and Apoptosis Assessment in Colonic Mucosa Using Flow Cytometry

Colonic epithelial and lamina propria fractions were isolated and sorted on FACS CANTO-II (BD BioSciences) from $Camp^{+/+}$ and $Camp^{-/-}$ mice (±*C. rodentium* at 7 dpi) as $CD326^+$ (563477; BD Biosciences) and $CD45^+$ (563891; BD Biosciences) cells, respectively. Lamina propria cells were further separated into $CD11b^+Ly6G^+$ (neutrophils) and $CD11c^+CX3CR1^+$ (resident macrophages). Both epithelial and lamina propria fractions were stained with anti-TOLLIP antibody (ab187198; Abcam; 1:100 dilution). TOLLIP expression data were represented as % $CD326^+$TOLLIP$^+$ (epithelial cells), % $CD45^+CD11c^+CX3CR1^+$TOLLIP$^+$ (macrophages), and % $CD45^+CD11b^+Ly6G^+$TOLLIP$^+$ (neutrophils). For apoptosis, cell fractions were analyzed upon staining with CD326, CD45, 7-AAD (559925; BD Biosciences), and annexin V (4830-01-K; Trevigen) antibodies, wherein early and late apoptotic cells were classified as annexin V^+7-AAD^- and annexin V^+7-AAD^+, respectively. Data were reported as % $CD326^+$annexin V^+7-AAD^- cells or % $CD326^+$annexin V^+7-AAD^+ of the total cell fraction. The representative gating strategy for TOLLIP expression in colonic epithelium, neutrophils, and macrophages is shown in online supplementary Figure S1 (for all online suppl. material, see www.karger.com/doi/10.1159/000526121).

pMIR-31-Luciferase Reporter Assay in Colonic Epithelium

HT29 cells were co-transfected with the pMIR-31-reporter plasmid (provided by Mien-Chie Hung, Addgene #71871) (1 μg) and constitutively luciferase-expressing pRL plasmid from *Renilla reniformis* (0.1 μg) in DMEM media (FBS and antibiotic free) using TransIT transfection reagent (MIR5405; Mirus Bio LLC). pRL null plasmid was used as transfection control. After overnight transfection, HT29 cells were treated as discussed above. Results were quantified using a dual luciferase reporter assay (PR-E1910; Promega). Data were calculated as inverse of firefly luciferase activity, normalized to control, and reported as % miR-31 expression for three independent experiments.

Shotgun Proteomics Analysis

Colons from *C. rodentium*-infected $Cramp^{+/+}$ and $Cramp^{-/-}$ mice were snap frozen in dry ice immediately after collection and stored at −80°C. Protein samples were lysed with 1% SDS (0227-100g; VWR), 0.1M EDTA (BDH9232-500g; VWR) in HEPES (200 nM, pH 8), and protease inhibitors (11836153001; Sigma). Proteins were denatured with 10 mM DTT, and cysteines were alkylated with 15 mM iodoacetamide (Rpn6302v; VWR) in dark for 25 min at RT with pH adjusted to 6.5 with HCl (46414-463; VWR). Samples were incubated with isotopically heavy formaldehyde (40 mM $13CD_2O$ + 20 mM $NaBH_3CN$ [sodium cyanoborohydride]) (41860-360; VWR) or light formaldehyde (40 mM light formaldehyde [CH_2O] + 20 mM $NaBH_3CN$) (1CCDLM4599-1MLOFS; ACP chemicals) (18 h, 37°C) and subjected to C18 chromatography before being subjected to liquid chromatography and tandem mass spectrometry (LC-MS/MS).

High-Performance Liquid Chromatography and Mass Spectrometry

Experiments were carried out using an Orbitrap Fusion Lumos Tribrid MS (Thermo Scientific) operated with Xcalibur (4.0.21.10) and coupled to a Thermo Scientific Easy-nLC (nanoflow liquid chromatography) 1,200 system (Southern Alberta Mass Spectrometry, Univ. Calgary). Tryptic peptides (2 μg) were loaded onto a C18 trap (75 μm × 2 cm; Acclaim PepMap 100, P/N 164946; Thermo Scientific) at a flow rate of 2 μL/min of solvent A (0.1% formic acid and 3% acetonitrile in LC-MS grade water). Peptides were eluted using a 120 min gradient from 5 to 40% (5–28% in 105 min followed by an increase to 40% B in 15 min) of solvent B (0.1% formic acid in 80% LC-MS grade acetonitrile) at a flow rate of 0.3 μL/min and separated on a C18 analytical column (75 μm × 50 cm; PepMap RSLC C18; P/N ES803; Thermo Scientific). Peptides were electrosprayed using 2.3 kV voltage into the ion transfer tube (300°C) of the Orbitrap Lumos operating in positive mode. The Orbitrap first performed a full mass spectrometry scan at a resolution of 120,000 FWHM to detect the precursor ion having an m/z between 375 and 1,575 and a +2 to +7 charge. The Orbitrap AGC (Auto Gain Control) and the maximum injection time were set at

4×10^5 and 50 ms, respectively. The Orbitrap was operated using the top speed mode with a 3 s cycle time for precursor selection. The most intense precursor ions presenting a peptidic isotopic profile and having an intensity threshold of at least 5,000 were isolated using the quadrupole and fragmented with HCD (30% collision energy) in the ion-routing multipole. Fragment ions (MS2) were analyzed in the ion trap at a rapid scan rate. The AGC and the maximum injection time were set at 1×10^4 and 35 ms, respectively, for the ion trap. Dynamic exclusion was enabled for 45 s to avoid acquisition of the same precursor ion with a similar m/z (±10 ppm).

Proteomic Data and Bioinformatics Analysis

Spectral data were matched to peptide sequences in the murine UniProt protein database using the Andromeda algorithm [57] as implemented in the MaxQuant [58] software package v.1.6.10.23, at a peptide-spectrum match FDR of <0.01. Search parameters included a mass tolerance of 20 ppm for the parent ion, 0.5 Da for the fragment ion; carbamidomethylation of cysteine residues (+57.021464 Da); variable N-terminal modification by acetylation (+42.010565 Da); and variable methionine oxidation (+15.994915 Da). N-terminal and lysine heavy (+34.063116 Da) and light (+28.031300 Da) dimethylation were defined as labels for relative quantification. The cleavage site specificity was set to Trypsin/P for the proteomics data, with up to two missed cleavages allowed. Significant outlier cutoff values were determined after $\log_{(2)}$ transformation by boxplot-and-whiskers analysis using the BoxPlotR tool. Changes in abundance of proteins as $\log_{(2)}$ (*Camp*$^{-/-}$ vs. *Camp*$^{+/+}$) means $\log_{(2)}$ values >0 represent proteins that were upregulated in *Camp*$^{-/-}$ and $\log_{(2)}$ values <0 proteins that were downregulated in *Camp*$^{-/-}$.

Statistical Analyses

Mice were randomly assigned to treatments with no criteria for inclusion or exclusion. Comparisons were done between *Camp*$^{+/+}$ and *Camp*$^{-/-}$ mice ± *C. rodentium* at 7 dpi. Analytical data represented as histograms were recorded as mean values with bars representing standard errors of the mean (SEM) from a minimum of three independent experiments, with data obtained in triplicate, unless stated otherwise. When possible, normality was assessed using Shapiro-Wilk (Royston) tests. All comparisons were performed using either a two-sided unpaired Student's *t* test or a one-way analysis of variance with a post hoc Bonferroni correction for multiple group comparisons or two-way analysis of variance. A *p* value was assigned to each group with reference to control group, unless shown specifically on the graph, and $p < 0.05$ was accepted as a statistically significant difference. All statistical analyses were performed with GraphPad Prism (v5.0).

Results

Cathelicidins Sustained TOLLIP Production in Colonic Epithelium from Mice Infected with C. rodentium*, Cultured Epithelia, and Colonoids*

Since cathelicidins modulate TLR responses in colonic epithelia [27, 59, 60], we investigated their possible impact on the TLR downstream effector, TOLLIP. While TOLLIP protein was minimally expressed in the colonic epithelium of noninfected *Camp*$^{+/+}$ and *Camp*$^{-/-}$ mice (Fig. 1a), *Camp*$^{+/+}$ mice infected with *C. rodentium* displayed abundant TOLLIP immunostaining at 7 dpi with marked expression in epithelial cells at the top of colonic crypts. These increases in TOLLIP abundance in response to *C. rodentium* did not occur in colons of *Camp*$^{-/-}$ mice (Fig. 1a). In addition, primary colonic epithelium isolated from *Camp*$^{+/+}$ mice revealed more immunoblotted TOLLIP protein compared to epithelia from *Camp*$^{-/-}$ colons (Fig. 1b, full blot in online suppl. Fig. S2A). Flow cytometry confirmed that colonic TOLLIP was present in CD326$^+$ epithelial cells during homeostasis and at 7 dpi with *C. rodentium*, with increased expression levels in *Camp*$^{+/+}$ mice (Fig. 1c). Intraperitoneal injection of synthetic murine cathelicidin (CRAMP; 8 mg/kg of body weight) before and during *C. rodentium* colonization (at −1, 1, 3, and 5 dpi) increased TOLLIP expression in CD326$^+$ epithelial cells of *Camp*$^{-/-}$ mice but had no significant effect in *Camp*$^{+/+}$ littermates (Fig. 1c). TOLLIP protein was also more abundant in *Camp*$^{+/+}$ bone marrow-derived macrophages under homeostasis (online suppl. Fig. S2B) and during *C. rodentium* infection (online suppl. Fig. S2C, D) in lamina propria CD45$^+$CD11b$^+$Ly6G$^+$ neutrophils (online suppl. Fig. S2C) and CD45$^+$CD11c$^+$CX3CR1$^+$ macrophages (online suppl. Fig. S2D) compared to *Camp*$^{-/-}$ cells. *TOLLIP* mRNA in the colonic epithelium was not different between *Camp*$^{+/+}$ and *Camp*$^{-/-}$ mice (online suppl. Fig. S2E), suggesting that cathelicidin-deficient mice have impaired colonic post-transcriptional synthesis of TOLLIP.

The mechanisms by which cathelicidins induce TOLLIP were studied in human colon-derived HT29 epithelial cells. Increasing concentrations of LL-37 (1–10 μg/mL, equivalent to 0.2–2 μM) or treatment times up to 8 h did not increase *TOLLIP* mRNA expression in HT29 cells (online suppl. Fig. S2F) but did increase TOLLIP protein abundance (Fig. 1d). HT29 cells exposed to high concentrations of LL-37 (e.g., 200 μg/mL) had reduced TOLLIP protein (online suppl. Fig. S3A), consistent with reports of cytotoxic effects of elevated doses of cathelicidins [61]. Colonic organoids from normal/control *Camp*$^{+/+}$ mice also showed increased TOLLIP protein levels following exposure to LL-37 (Fig. 1e). LL-37 increased TOLLIP protein in murine adipose-derived (L929) fibroblasts (online suppl. Fig. S3B).

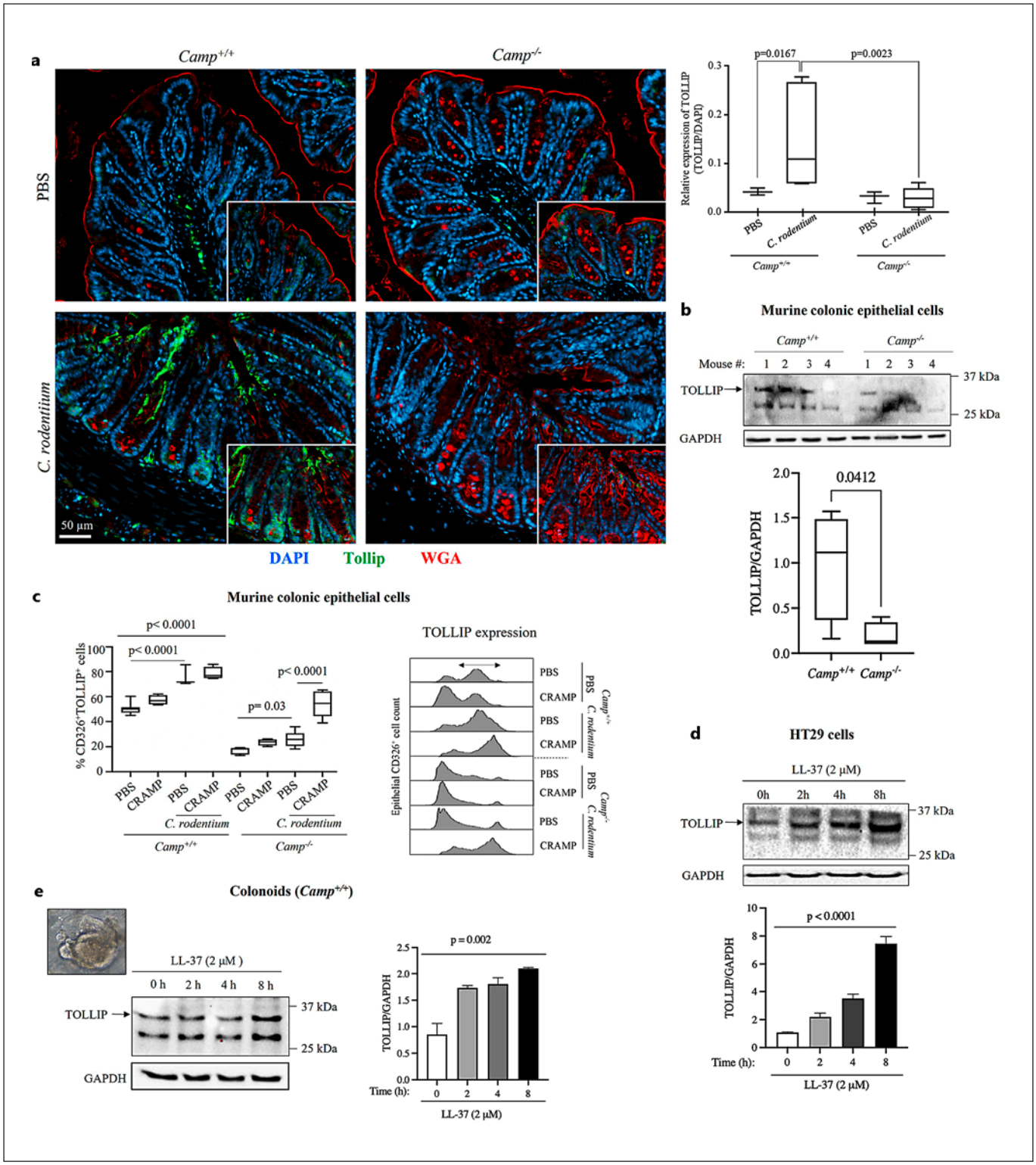

1

(For legend see next page.)

Cathelicidin-Upregulated TOLLIP Prevented IRAK-1 Phosphorylation and Pro-Inflammatory Cytokine Synthesis in Colonic Epithelium

Because TOLLIP prevents phosphorylation to inhibit IRAK-1/NF-κβ signaling in macrophages [39, 62, 63], we investigated if the TLR-IRAK-1 axis in colonic epithelia was impacted by the ability of cathelicidin to increase TOLLIP. On average, phospho-IRAK-1 was reduced in primary colonic epithelial cells from *Camp*$^{+/+}$ mice compared to those from *Camp*$^{-/-}$ littermates (Fig. 2a). Pretreatment with LL-37 prevented phosphorylation of IRAK-1 in LPS-stimulated HT29 cells (Fig. 2b). To determine if cathelicidins reduce IRAK-1 activation through TOLLIP, endogenous LL-37 and TOLLIP were silenced in HT29 cells (knockdown efficiency ~90% for LL-37 (online suppl. Fig. S3C) and TOLLIP (online suppl. Fig. S3D) cells. Both shLL-37 and shTOLLIP HT29 cells expressed higher basal phospho-IRAK-1 compared to sham-transfected HT29 cells (Fig. 2c).

We next evaluated if LL-37 regulates inflammatory signaling directly through TOLLIP. shTOLLIP HT29 cells stimulated with LL-37 had increased expression of *IFNγ*, *TNFα*, and *IL1β* mRNA, but the responses were lesser compared with TOLLIP-expressing sham-transfected HT29 cells (Fig. 2d). Regardless of TOLLIP availability, secretion of CXCL1, IL10, IL8 and production of IL1Rα remained unaffected post-LL-37 treatment (for up to 16 h) (online suppl. Fig. S3E). Collectively, the data indicate that cathelicidins via TOLLIP inhibition of phospho-IRAK-1 in colonic epithelia limit the synthesis of proinflammatory cytokines.

Cathelicidins Induced Trans-Activation of Epidermal Growth Factor Receptor (EGFR) in Colonic Epithelium

To assess mechanisms of TOLLIP regulation, cell surface receptors previously implicated in mediating cathelicidin's effect on enterocytes and leukocytes were examined, namely, EGFR, FPR2, and P2X7 [19]. Blocking of EGFR phosphorylation/activation with the EGF kinase inhibitor, AG1478, reduced LL-37-induced expression of TOLLIP, whereas FPR2- or P2X7-selective inhibitors did not alter the LL-37 effect (Fig. 3a). A scrambled peptide sequence of LL-37 (sLL-37) did not affect TOLLIP abundance (Fig. 3a). Furthermore, LL-37 increased phospho-EGFR in HT29 cells (Fig. 3b). Primary colonic epithelium from *Camp*$^{+/+}$ mice displayed higher constitutive phospho-EGFR compared to cells from *Camp*$^{-/-}$ mice (Fig. 3c).

Cathelicidins Inhibited miRNA-31 to Increase TOLLIP and Regulate RNA Silencing Dicer Argonaute 2 (AGO2)

In the absence of evidence that cathelicidins alter TOLLIP gene transcription (online suppl. Fig. S2E, F), post-transcriptional regulation was considered. We focused on miR-31, a single-stranded non-coding RNA that cleaves mRNA targets [64] and represses TOLLIP expression in enteric epithelia [65] and THP-1 monocytes [66]. Stimulation of HT29 cells with LL-37 reduced the gene expression (Fig. 4a) and activity of miR-31 as determined in a luciferase reporter assay (Fig. 4b). The reduced gene expression of miR-31 by LL-37 in HT29 cells was abrogated by co-treatment with the EGFR kinase inhibitor, AG1478 (Fig. 4c). Overexpression of miR-31 in HT29 cells (~3-fold) (online suppl. Fig. S3F) prevented LL-37-induced

Fig. 1. Cathelicidins upregulate TOLLIP abundance in colonic epithelium. *Camp*$^{+/+}$ and *Camp*$^{-/-}$ mice were given *C. rodentium* (~5 × 10^8 CFU in 200 μL of PBS) or PBS by oral gavage. **a** TOLLIP immunostaining in colons showing abundant expression in *Camp*$^{+/+}$ colonic epithelium at the top of the crypts (7 days postinfection), while *Camp*$^{-/-}$ mice did not produce TOLLIP in response to *C. rodentium*. Images were taken with a ZEISS AXIO microscope (20X, NA 0.5) and analyzed by ZEN 2.6 (2018) software. Fluorescent TOLLIP (green) was calculated using ImageJ 1.53c software (National Institute of Health, USA) and represented as mean fluorescence intensity (MFI). Data are shown as means ± SEM (n = 3–7 mice/group) and analyzed by Kruskal-Wallis test for mean comparison and Mann-Whitney U test. $p < 0.05$ was considered significant. **b** TOLLIP synthesis in colonic epithelial cells of *Camp*$^{+/+}$ and *Camp*$^{-/-}$ mice determined by Western blotting (n = 4 mice/group, numbered at top), and the corresponding bar graph depicting quantification of the blot after normalization to GAPDH. **c** Flow cytometry analysis of TOLLIP expression in primary colonic epithelial (CD326$^+$) cells isolated from *Camp*$^{+/+}$ and *Camp*$^{-/-}$ mice infected with *C. rodentium* and ip. injected with synthetic CRAMP (8 μg/body weight g; −1-, 1-, 3-, and 5-days postinfection). The staggered histogram shows cell counts on the y-axis and TOLLIP protein synthesis intensity on x-axis. The bi-directional arrow on the top of the second peak on histogram represents cell population with increased TOLLIP protein synthesis. **d**, **e** TOLLIP quantification in (**d**) HT29 cells and (**e**) *Camp*$^{+/+}$ colonoids stimulated with LL-37 (2 μM; for up to 8 h) determined by Western blotting with corresponding bar graphs depicting quantification of the blots after normalization to GAPDH. Blots are representative of 3 independent experiments with comparable results. Data are mean ± SEM. $p < 0.05$ (two-way ANOVA or one-way ANOVA post hoc Bonferroni correction for multiple group comparison) was considered significant.

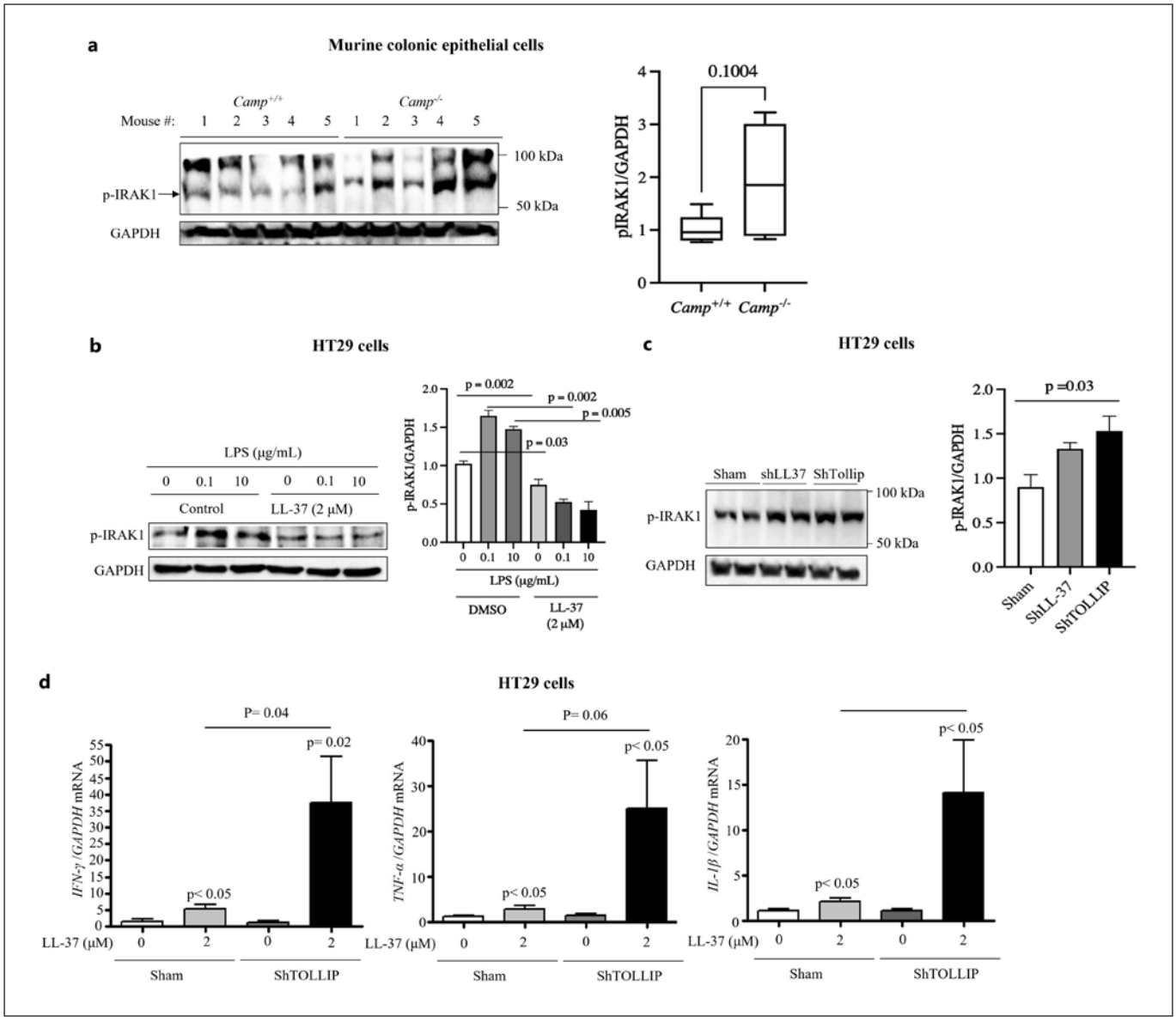

Fig. 2. Cathelicidins prevent IRAK-1 phosphorylation and proinflammatory cytokine expression in colonic epithelium via TOLLIP. **a** Constitutive IRAK-1 phosphorylation (pIRAK-1) in primary colonic epithelial cells isolated from *Camp*$^{+/+}$ and *Camp*$^{-/-}$ mice determined by Western blotting (n = 5 mice/group, numbered at top). **b**, **c** IRAK-1 phosphorylation (pIRAK) in (**b**) wild-type HT29 cells and (**c**) HT29 cells sham transfected or knocked-down for endogenous LL-37 (shLL37) or TOLLIP (shTOLLIP) stimulated by (**b**) LL-37 (2 μM; 8 h) or (**c**) nonstimulated after challenge with (**b**) LPS (0.1 or 10 μg/mL; 2 h) or (**c**) inert control (sham) determined by Western blotting. **a–c** Relative pIRAK:GAPDH signal ratios obtained by densitometry with corresponding bar graphs depicting quantification of the blots after normalization to GAPDH. **b**, **c** Blots are representative of three independent experiments with comparable results. **d** mRNA expression of IFNγ, TNFα, and IL1β in HT29 cells either wild-type (sham) or sh-down-regulated TOLLIP (shTOLLIP) cells upon treatment with LL-37 (2 μM, 16 h) determined by qPCR. Data were represented relative to GAPDH. Data are means ± SEM. $p < 0.05$ (one-way ANOVA post hoc Bonferroni correction for multiple group comparison or two-tailed Student's t test for 2 groups) was considered significant.

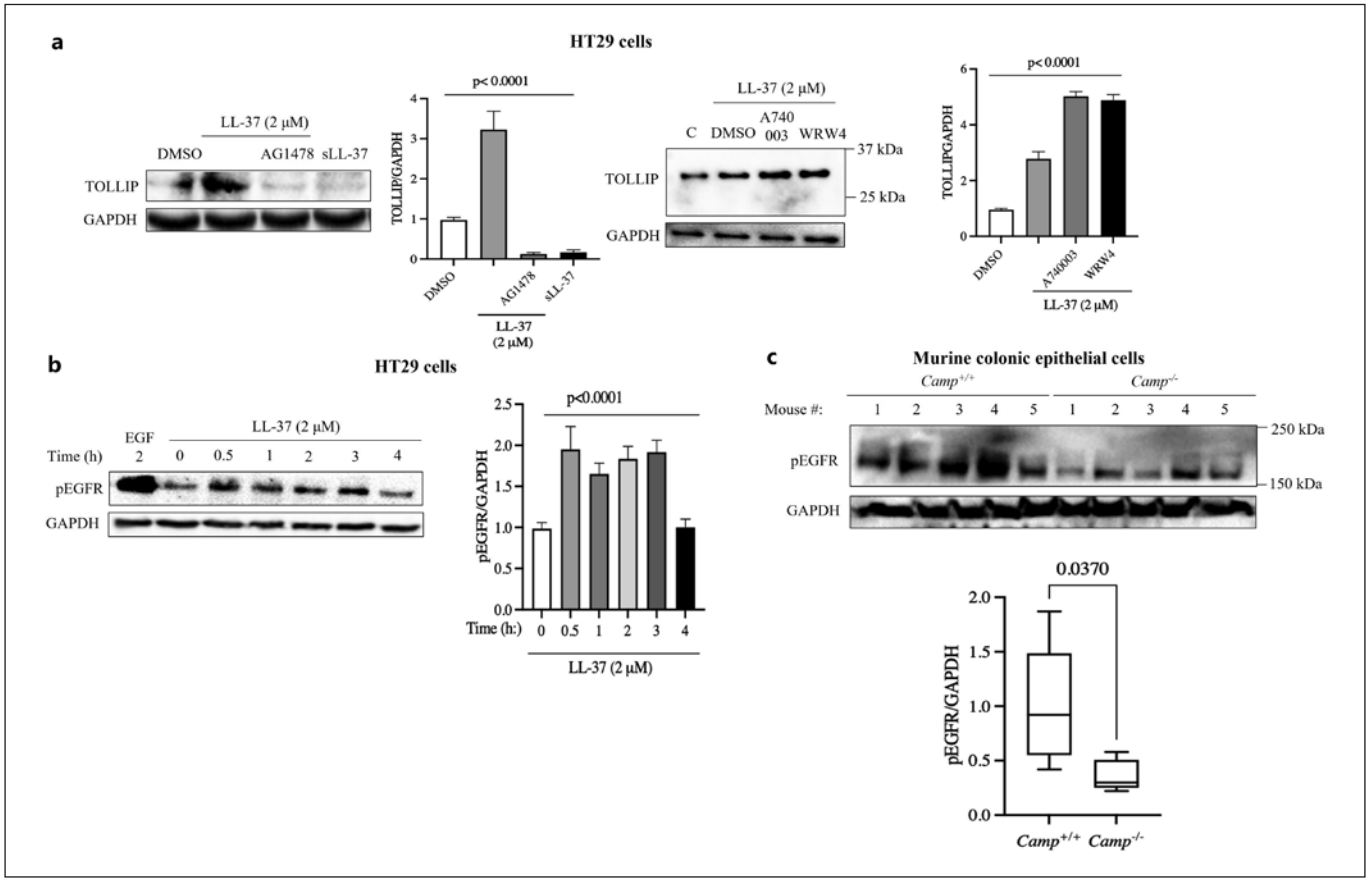

Fig. 3. Cathelicidins induce colonic TOLLIP upregulation via EGFR activation-phosphorylation. **a** TOLLIP protein synthesis in HT29 cells pretreated with chemical inhibitors/antagonists for EGFR kinase (AG1478; 1 μM), formyl peptide receptor-like-1 (WRW4; 10 μM), purinergic P2X7 receptor (A740003; 10 μM), or DMSO vehicle (1 h), followed by treatment with LL-37 (2 μM) or scrambled LL-37 peptide (sLL37, 2 μM; 8 h) determined by Western blotting. Data were represented relative to the GAPDH signal by densitometry. Blots are representative of 3 independent experiments with comparable results. **b** EGFR phosphorylation-activation in HT29 cells upon treatment with LL-37 (2 μM) for variable times (top of blot) determined by Western blotting. Synthetic EGF (1 ng/mL; 2 h) was used as a positive control. Blots are representative of 3 independent experiments with comparable results. **c** Spontaneous EGFR phosphorylation in primary colonic epithelial cells isolated from *Camp*$^{+/+}$ and *Camp*$^{-/-}$ mice (n = 5 mice/group, numbered at top) determined by Western blotting. **a–c** Corresponding bar graphs depicting quantification of the blots after normalization to GAPDH illustrated next to the blots. Data are mean ± SEM. $p < 0.05$ (two-way ANOVA or one-way ANOVA post hoc Bonferroni correction for multiple group comparison) was considered significant.

TOLLIP upregulation (Fig. 4d). Primary colonic epithelia from *Camp*$^{+/+}$ mice showed lower miR-31-5p expression compared to *Camp*$^{-/-}$ littermates (Fig. 4e). We next tested whether TOLLIP degradation in the absence of LL-37 was through proteosome activity. While LL-37 alone enhanced TOLLIP synthesis in HT29 cells, the proteosome inhibitor, MG132, prevented the stimulatory effect of cathelicidin; then, TOLLIP expression remained at control levels (Fig. 4f).

To further explore the role of cathelicidins in TOLLIP RNA silencing, a shotgun proteomic profile of colons from *Camp*$^{+/+}$ and *Camp*$^{-/-}$ mice infected with *C. rodentium* (7 dpi) was conducted (online suppl. Fig. S4). Colons from *C. rodentium*-infected *Camp*$^{-/-}$ mice had increased expression of proteins involved in RNA silencing and mRNA metabolic processing pathways (online suppl. Fig. S4). Specifically, *C. rodentium*-infected *Camp*$^{-/-}$ colons showed dicer Argonaute 2 (AGO2), a protein that cleaves pre-miRNAs, in association with the functionally related proteins, mRNA repressive Y-box-binding protein (Ybx3), zinc finger CCCH-type containing antiviral (Zc3hav) 1, polyadenylate-binding nuclear protein (Pabpn) 1, and tudor domain containing (Tdrd) 1 (online suppl. Fig. S4; Table 1). Subsequently, LL-37 increased phos-

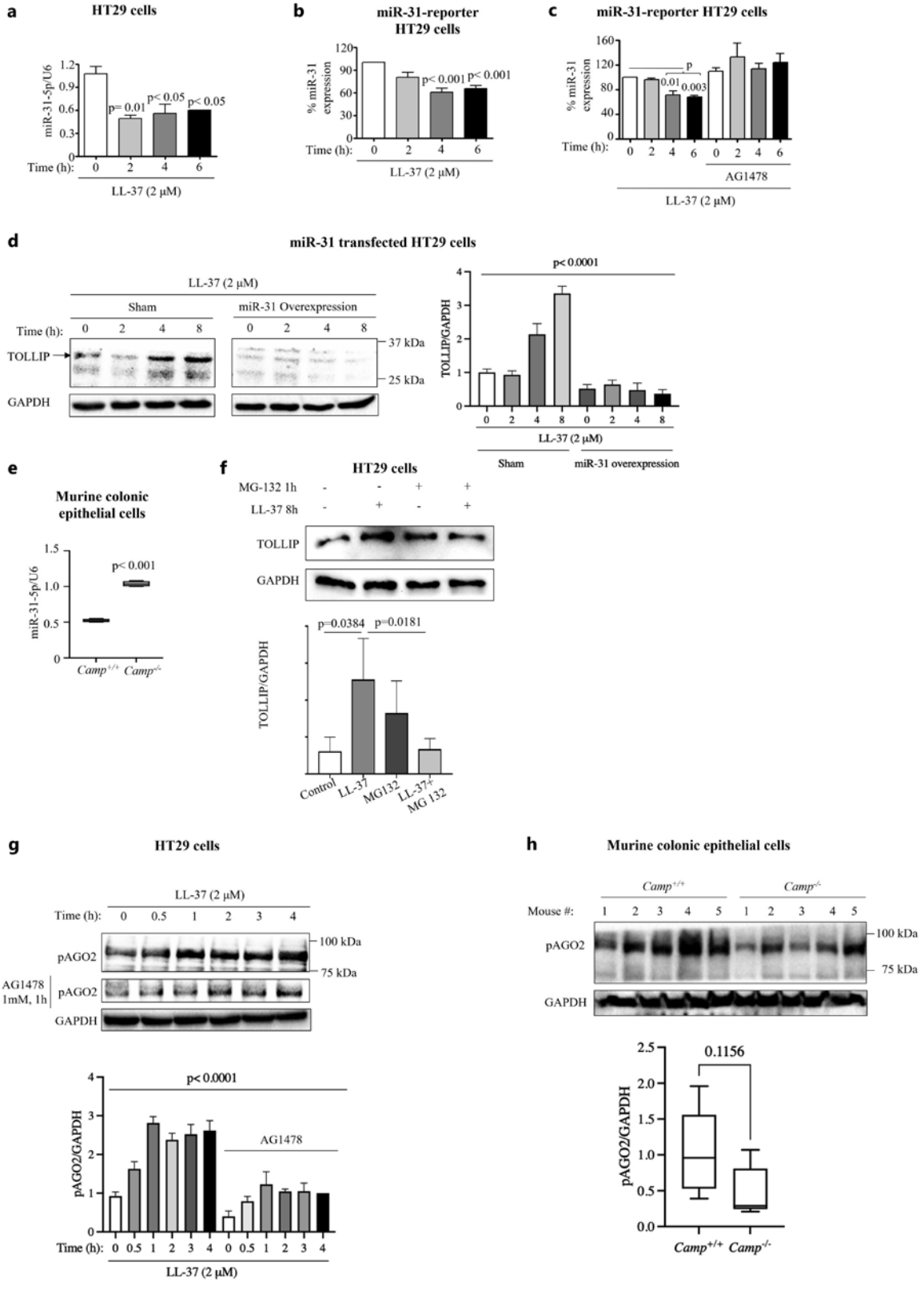

4

(For legend see next page.)

pho-AGO2 expression in HT29 cells, an effect abrogated by AG1478 (Fig. 4g). Isolated colonic epithelia from *Camp*$^{+/+}$ mice revealed increased phospho-AGO2 compared to those from *Camp*$^{-/-}$ mice (Fig. 4h). Thus, cathelicidins could lower miR-31 levels in colonic epithelium by activation of its negative regulator, AGO2.

TOLLIP Upregulated by Cathelicidins Decreased TNFα/Ifnγ-Induced Epithelial Apoptosis

Since LL-37 prevents apoptosis in endothelial cells [67] and neutrophils [68], and TOLLIP signaling is associated with apoptosis suppression in bronchial [69] and colonic epithelia [43], we sought to determine if a functional impact of cathelicidin induction of TOLLIP is increased epithelial survival. Both *Camp*$^{+/+}$ and *Camp*$^{-/-}$ mice showed comparable overall numbers of apoptotic cells in distal colons at 7 and 14 dpi with *C. rodentium* as determined by TUNEL assay (online suppl. Fig. S5A, B). However, the number of early and late apoptotic CD326^{+} epithelial cells increased in colons of both *Camp*$^{+/+}$ and *Camp*$^{-/-}$ mice at the peak of *C. rodentium*-induced colitis (i.e., 7 dpi), but it was higher in *Camp*$^{-/-}$ mice (Fig. 5a). Furthermore, *Camp*$^{-/-}$ epithelial cells were more sensitive to apoptosis, as gauged by higher levels of cleaved caspase-3 and PARP compared with *C. rodentium*-infected *Camp*$^{+/+}$ epithelia (Fig. 5b). To determine if the prevention of apoptosis by cathelicidins is dependent on TOLLIP, shTOLLIP HT29 cells were treated with TNFα (100 ng/mL) + IFNγ (300 IU/mL) to induce apoptosis (Fig. 5c, d). LL-37 reduced caspase-3 and PARP cleavage (Fig. 5c) and LDH release (Fig. 5d) in sham-transfected HT29 cells but not in TOLLIP-silenced cells. The proteomic analysis of *C. rodentium*-infected *Camp*$^{+/+}$ colons (7 dpi) demonstrated enrichment for peroxisome proliferator-activated receptor (PPAR) signaling pathways (online suppl. Fig. S4), associated with apoptosis, differentiation, and cell cycle arrest [70, 71]. Moreover, single protein resolution analysis in *C. rodentium*-infected *Camp*$^{-/-}$ colons compared to *Camp*$^{+/+}$ showed an increase in the proapoptotic factor, serine/threonine-protein kinase (PRKC) apoptosis WT1 regulator protein (PAWR) ($\log_{(2)}$ value 1.94) and a decrease in the anti-apoptotic protein, apoptosis antagonizing transcription factor (AATF) ($\log_{(2)}$ value −6.8) (Table 1). Thus, we surmise that cathelicidins might sustain the lifespan of colonic epithelium via TOLLIP.

Discussion

This study establishes that cathelicidins regulate TLR signaling in colonic epithelium by sustaining TOLLIP, a negative TLR/IRAK-1/NF-kβ adapter [39]. Moreover, cathelicidin-mediated maintenance of TOLLIP, via EGFR activation and reduction of miR-31, reduces the synthesis of proinflammatory cytokines and enhances cell survival in colonic epithelia. These findings underscore the anti-inflammatory capacity of LL-37 [4], many of which converge on regulation of the TLR4/TRL2/1-NF-kβ axis [21, 25, 26, 72–74] and denote the importance of this peptide in mobilizing epithelial innate defenses [27]. In accordance with the data herein, TOLLIP has been found to inhibit LPS-mediated IRAK-1 phosphorylation in embryonic kidney epithelial (HEK293) cells [62] and nitric oxide synthase-mediated NO/COX2 and IL8 production in HT29 cells [75]. Moreover, TOLLIP reduces secretion

Fig. 4. Cathelicidins promote colonic TOLLIP expression via proteosome activation, EGFR-mediated AGO2 phosphorylation, and downregulation of miR-31. **a** miR-31 quantification in HT29 cells stimulated with LL-37 (2 μM) for the stated times by qPCR. Data are represented as fold change relative to LL-37. U6 snRNA was used to normalize the miRNA-31 signal. **b**, **c** miR-31 expression in HT29 cells (**b**) untreated or (**c**) pretreated with EGFR kinase inhibitor (AG1478; 1 μM, 1 h) stimulated with LL-37 (2 μM) determined by luciferase assay. Luciferase signal was calculated as the inverse of luciferase activity normalized to constitutive luciferase activity of pRL null plasmid used as transfection control. **d** TOLLIP protein synthesis in HT29 cells transfected with empty vector (sham) or a miR-31 overexpression plasmid (**d**) stimulated with LL-37 (2 μM) determined by Western blotting and represented relative to the GAPDH signal. **e** miR-31 expression in primary colonic epithelial cells isolated from *Camp*$^{+/+}$ and *Camp*$^{-/-}$ mice (n = 4–5 mice/group) quantified by qPCR and normalized using U6 snRNA. **f** TOLLIP protein synthesis in HT29 cells pretreated with the proteosome inhibitor (MG132; 10 μM, 1 h) stimulated with LL-37 (2 μM; 8 h) determined by Western blotting and represented relative to the GAPDH signal. **g** Time course of AGO2 phosphorylation-inactivation (pAGO2) in HT29 cells ± EGF kinase inhibitor (AG1478; 1 mM, 1 h pretreatment) determined by Western blotting and represented relative to the GAPDH signal. **h** AGO2 phosphorylation-inactivation in *Camp*$^{+/+}$ and *Camp*$^{-/-}$ mice assessed by Western blotting and normalized to the GAPDH signal (n = 5 mice/group). **b**, **f**–**h** Corresponding bar graphs depicting quantification of the blots after normalization to GAPDH illustrated next to the blots. **b**, **f**–**g** Blots were representative of 3 independent experiments with comparable results. Data are mean ± SEM. $p < 0.05$ (two-way ANOVA or one-way ANOVA post hoc Bonferroni correction for multiple group comparison) was considered significant.

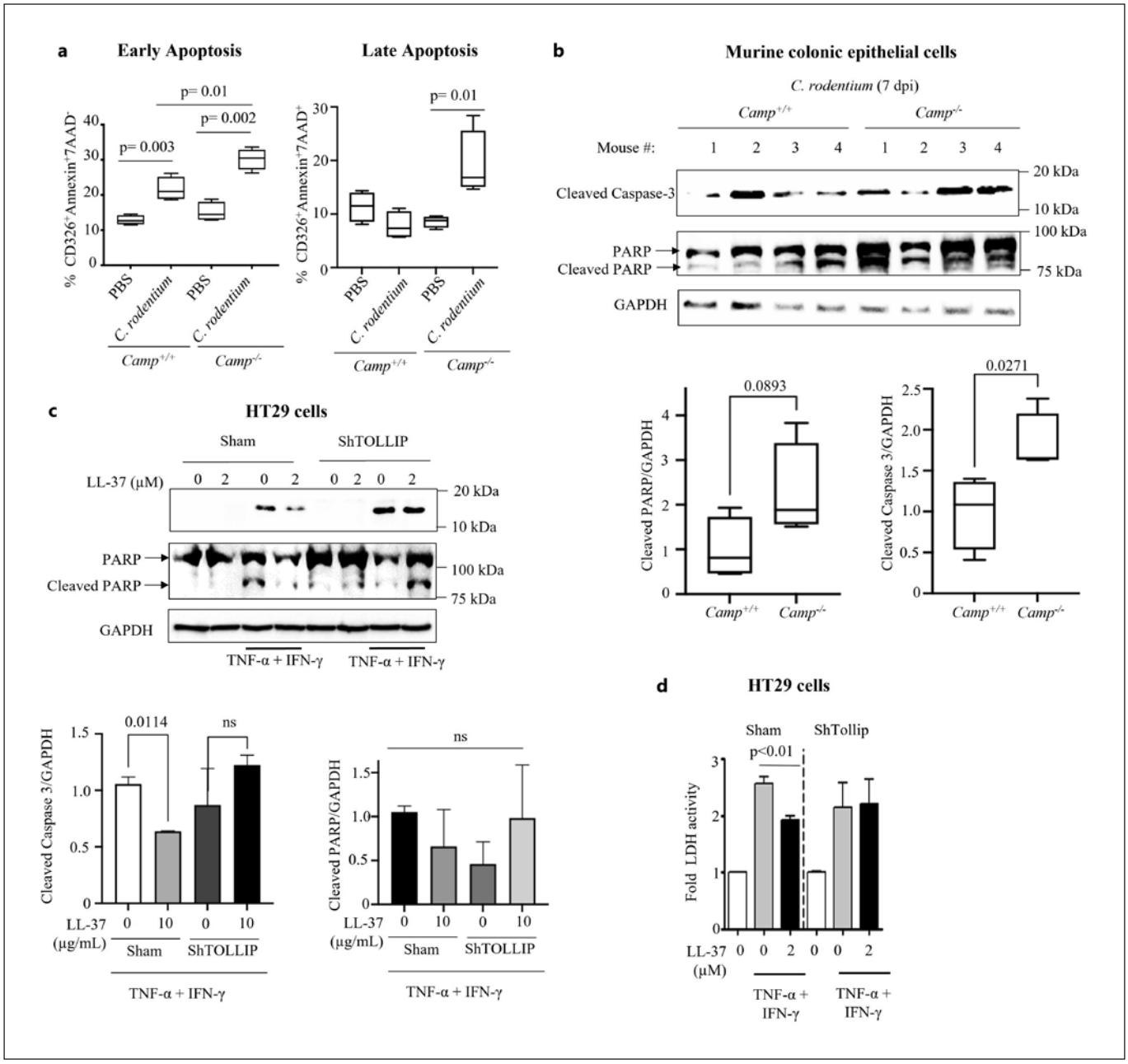

Fig. 5. Cathelicidins prevent *C. rodentium*-induced apoptosis in murine colonic epithelium and cytokine-induced apoptosis in HT29 cells via TOLLIP. **a** Flow cytometry analysis of colonic CD326$^+$ "early apoptotic" (Annexin$^+$ 7AAD$^-$) and "later apoptotic" (Annexin$^+$7AAD$^+$) epithelial cells and (**b**) cleaved caspase-3 and PARP in colonic epithelium from *Camp*$^{+/+}$ and *Camp*$^{-/-}$ mice infected with *C. rodentium* at 7 days postinfection (n = 4 mice/group, numbered at top) analyzed by Western blotting. GAPDH was used as a housekeeping control. **c** Cleaved caspase-3 and PARP determined by Western blotting and (**d**) cell death analyzed by LDH activity in supernatant from HT29 cells pretreated with LL-37 (10 μg/mL; 8 h) followed by a combination of TNFα (100 ng/mL) and IFNγ (300 U/mL) for 16 h. **b**, **c** Corresponding bar graphs depicting quantification of the blots after normalization to GAPDH illustrated next to the blots. Data are mean ± SEM. $p < 0.05$ (one-way ANOVA post hoc Bonferroni correction for multiple group comparison or two-tailed Student's t test for two groups) was considered significant.

Table 1. Major protein hits identified in upregulated mRNA metabolic process pathways from *C. rodentium*-infected *Camp*$^{-/-}$ colons and involvement in different biological processes

Protein name	Gene name	Log_2 (*Camp*$^{-/-}$: *Camp*$^{+/+}$)	Biological process (GO)
KH domain-containing, RNA-binding, signal transduction-associated protein 3	Khdrbs3	5.91	Positive regulation of RNA splicing; regulation of alternative mRNA splicing, via spliceosome; regulation of mRNA splicing, via spliceosome
Pinin	Pnn	1.64	RNA splicing; mRNA processing; cell-cell adhesion
Splicing factor 3A subunit 2	Sf3a2	3.49	U2-type pre-spliceosome assembly; spliceosomal complex assembly; ribonucleoprotein complex assembly
Polyadenylate-binding protein 2	Pabpn1	1.79	Positive regulation of polynucleotide adenylyltransferase activity; regulation of polynucleotide adenylyltransferase activity; poly(A)+ mRNA export from nucleus
WD40 repeat-containing protein SMU1; WD40 repeat-containing protein SMU1, N-terminally processed	Smu1	1.83	RNA splicing, via transesterification reactions; RNA splicing, via transesterification reactions with bulged adenosine as nucleophile; mRNA splicing, via spliceosome
Survival of motor neuron-related-splicing factor 30	Smndc1	1.66	RNA splicing; mRNA processing; mRNA metabolic process
Zinc finger CCCH-type antiviral protein 1	Zc3hav1	2.26	Positive regulation of RIG-I signaling pathway; cellular response to exogenous dsRNA; regulation of RIG-I signaling pathway
AHNAK nucleoprotein 2	Ahnak2	1.66	Regulation of RNA splicing; regulation of RNA metabolic process; regulation of nucleobase-containing compound metabolic process
Plakophilin-3	Pkp3	1.61	Desmosome assembly; desmosome organization; negative regulation of mRNA catabolic process
MKIAA3013 protein	Scaf11	1.79	Spliceosomal complex assembly; ribonucleoprotein complex assembly; ribonucleoprotein complex subunit organization
Protein Argonaute-2	Ago2	1.82	Regulation of translation, ncRNA mediated; positive regulation of translation, ncRNA mediated; mRNA destabilization-mediated gene silencing by siRNA

of IL6, TNFα, and IFNβ in murine macrophages [76] and abolishes inflammatory signaling in murine medullary thick ascending limbs [77]. Given the immunoregulatory characteristics of TOLLIP-driven LPS-TLR signaling, cathelicidins may contribute to gut hypo-responsiveness to LPS to limit exaggerated inflammatory responses.

Here, cathelicidins promoted post-transcriptional synthesis of TOLLIP in colonic epithelium independent of de novo transcription, and a similar uncoupling of TOLLIP mRNA and protein synthesis was reported in murine colon but not small bowel extracts [65]. Our data in primary murine colonic epithelium and human epithelial HT29 cells showed cathelicidins increased TOLLIP via phosphorylation of EGFR, although LL-37-treated epithelia did not produce measurable amounts of released EGF (data not shown). In accordance, LL-37 alone has no effect on EGFR phosphorylation [78] and CRAMP fails to interact with EGFR in vitro [79], but combined with LPS, LL-37 activates EGFR in colonic epithelium [27]. LL-37 induces EGFR phosphorylation in keratinocytes [80, 81]. The mechanism of EGFR activation by cathelicidins awaits elucidation, although it likely occurs via intracellular receptor transactivation due to perturbation in cholesterol-rich lipid raft domains in the plasma membrane [27]. Supporting this assumption, cholesterol depletion in the fibroblast plasmalemma induces EGFR activation in a ligand-independent manner [82].

The effect of cathelicidins on TOLLIP via EGFR elicited AGO2 phosphorylation while reducing mature miR-31 (miR-31-5p). A crosstalk between EGFR and AGO2 could regulate miR processing as EGFR signaling has been shown to increase miR-21 in the human bronchial epithelial (HBET2) cell line [83], and AGO2 ablation increases phospho-EGFR and mature miRs in murine pancreas [84, 85]. Conversely, EGFR phosphorylates AGO2 and reduces miR-31-5p expression in hypoxic HeLa cells

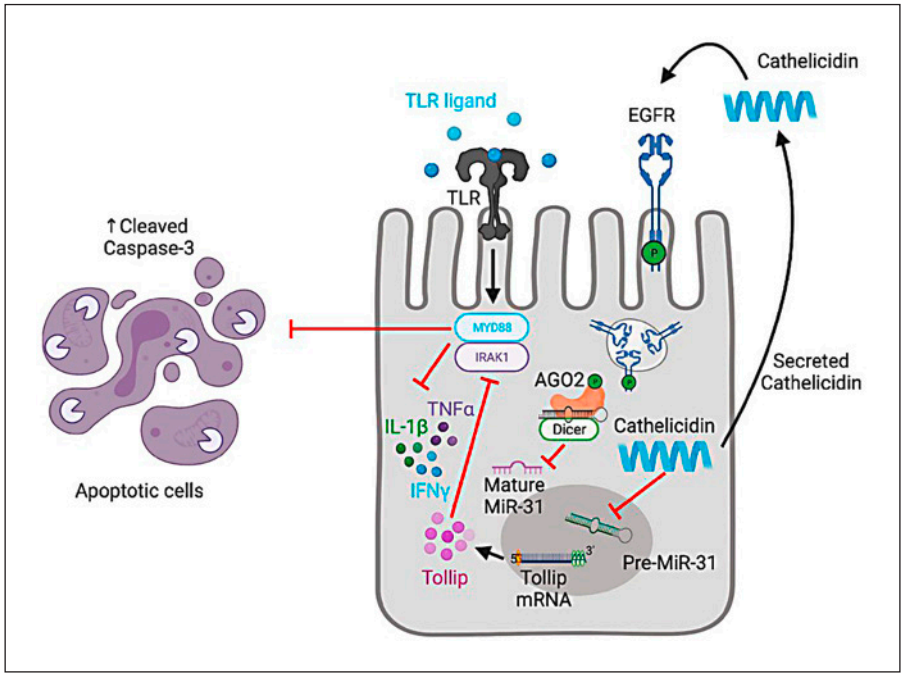

Fig. 6. Hypothetical scheme of signaling mechanisms elicited by cathelicidins to sustain TOLLIP synthesis in colonic epithelium. Cathelicidins activate intracellularly EGFR in colonic epithelial cells and promote phosphorylation of AGO2. This action inactivates AGO2 and the maturation of miR-31. Non-functional miRNA-31 is not available to promote catalytic degradation of TOLLIP and thus sustained TOLLIP synthesis occurs. TOLLIP suppresses TLR/MYD88/IRAK-1 signaling and the synthesis of proinflammatory cytokines (IFNγ, TNFα, IL1β) and promotes cell survival by inhibiting apoptosis.

[86], and EGFR signaling downregulates miR-143/145 expression in colonic tumors [87]. Phosphorylation of AGO2 causes its degradation or inactivation [88, 89], and hence, cathelicidins by transactivating the EGFR could suppress AGO2 activity. Indeed, we detected abundant AGO2 protein in colons of *C. rodentium*-infected *Camp*$^{-/-}$ mice compared to *Camp*$^{+/+}$ mice. Since EGFR inhibits miRNA maturation through phosphorylation of AGO2 in hypoxic breast cancer cells [86], cathelicidin-evoked phosphorylation of AGO2 via EGFR would inactivate AGO2 and repress miRNA-31 maturation (Fig. 6). Repression in miR levels can occur through an ubiquitin-proteasome pathway [90], and use of MG132 indicates a role for the proteosome machinery in cathelicidin preservation of TOLLIP protein stability in colonic epithelia. Further studies should elucidate additional aspects of the mechanism of cathelicidins maintenance TOLLIP, including direct phosphorylation of tyrosine-kinase substrates, for example, TOLLIP by EGF [91] and phosphorylation of TOLLIP-associated Tom1L1 proteins [92, 93].

The proposed link between cathelicidins and TOLLIP with miR-31-5p could be important in the regulation of inflammation. Reduced miR-31-5p expression is associated with enhanced TOLLIP in murine colons [65], and an LL-37 analog, FF/CAP18, provokes secretion of exosomes containing miR-31-5p from human colonic epithelial (HCT116) cells [94]. In addition, cathelicidin and miRNAs might act reciprocally, since LL-37 increases miR200c-3p levels in HT29 cells, whereas overexpression of miR-130a in murine bone-marrow derived mononuclear cells reduces *Camp* expression [95, 96]. Administering CRAMP at doses shown to protect mice from infectious [48, 49] and abiotic [50] colitis and auto-inflammatory diseases [51, 52] partially replenished colonic expression of TOLLIP in *C. rodentium*-infected *Camp*$^{-/-}$ mice. But naive mice treated with CRAMP showed unaltered TOLLIP protein synthesis. These data are consistent with the earlier finding that LPS is critical for cathelicidin induction of colonic epithelial cytokine production [27].

Colitis evoked by attaching/effacing enteropathogens has been associated with colonic epithelial damage [97, 98] and apoptosis due to aberrant TLR signaling and exaggerated release of proinflammatory cytokines [99–101]. Although the antiapoptotic role of cathelicidins is not yet fully understood, low concentrations of LL-37 (~1 μg/mL) prevent LPS-induced apoptosis in murine endothelial cells [67] and enhance expression of the antiapoptotic signal, Bcl-x(L), in human neutrophils [68]. Our data indicate that cathelicidins, via TOLLIP, sustain colonic epithelial cell survival in the face of challenge with IFNγ and TNFα, and in *C. rodentium*-evoked murine colitis. Moreover, apoptotic caspase-3 and PARP proteins along with early apoptotic colonic epithelial cells pre-

vailed in *Camp*$^{-/-}$ mice after infection with *C. rodentium*. Lack of differences between *C. rodentium*-infected *Camp*$^{-/-}$ and *Camp*$^{+/+}$ mice in TUNEL^{+} cells via microscopical quantification likely correspond to excessive epithelial cells lost in *Camp*$^{-/-}$ mice during infection as apoptotic colonic epithelium can be shed into the intestinal lumen during *C. rodentium* infection [102]. In concordance with our data, endogenous TOLLIP reduces intestinal epithelial apoptosis in response to DSS [42, 103] and downregulates apoptosis-related genes in mice during early tumorigenesis [43]. Similarly, our proteomic analysis revealed higher expressions of apoptosis-inducing effectors, such as PARP13, in *C. rodentium*-infected *Camp*$^{-/-}$ colons compared to *Camp*$^{+/+}$ mice. PARP13 RNA-binding protein regulates mRNA stability and counteracts TNF-related apoptosis-inducing ligand (TRAIL) R4, a decoy receptor for TRAIL [104]. Moreover, PPAR, abundant in *C. rodentium*-infected *Camp*$^{+/+}$ colons, has been associated with cell lifespan [70, 71] and induces colon epithelial cell survival via vascular endothelial growth factor (VEGF) signaling pathways [105]. Proteomic analysis in *C. rodentium*-infected *Camp*$^{-/-}$ mice also showed higher caspase-8 protein, a downstream effector in extrinsic apoptosis triggered by TNFα + IFNγ [106]. Other post-transcriptional effects on cathelicidins could further mitigate LPS-TLR4 signaling, including the citrullination of arginine residues in LL-37 that decreases its affinity for LPS [107].

In summary, while concentrations of cathelicidins as high as 300 μM have been reported in cases of atopic dermatitis, pneumonia, or systemic infection in newborn infants [12], we present evidence that lower, physiologically relevant levels of cathelicidins (i.e., <2–4 μM) limit proinflammatory cytokine production by colonic epithelia and promote cell survival. Mechanistically, these events require EGFR activation and reduced miR-31 to sustain TOLLIP protein, which in turn reduces IRAK-1 activation.

Acknowledgments

Immunofluorescence studies were conducted in the Live Cell Imaging Facility, The Clavin, Phoebe and Joan Snyder Institute for Chronic Diseases, Univ. Calgary. Proteomic studies were conducted in the Centre for Advanced Technologies (CAT) in the Cumming School of Medicine, Univ. Calgary. Organoids were provided by the Snyder Institute Human Organoid Innovation Hub, Univ. Calgary.

Statement of Ethics

The animal study protocol was reviewed and approved by the Canadian Guidelines for Animal Welfare (CGAW) and the University of Calgary Animal Care Committee (AC20-0050).

Conflict of Interest Statement

The authors have no conflicts of interest to declare.

Funding Sources

This work was supported by an NSERC Discovery Grant (RGPAS-2017-507827), Alberta Government Major Innovation Fund (RCP-19-003-MIF), and Alberta Agriculture and Forestry (2018F050R, 2019F041R).

Author Contributions

R.H. performed the in vitro and in vivo experiments, acquisition, analysis of data, and prepared the figures. C.R. contributed to the apoptosis assessment. A.B. conducted mice infection and flow cytometry studies in epithelial and lamina propria cells. G.A.D.B. participated in mice infection, PCR experiments, and manuscript editing. P.L., D.Y., and A.D. contributed to the proteomic analysis. M.D.H. participated in conceiving the experiments, edited the manuscript, and contributed reagents, materials, and analysis tools. R.H., D.M.M., and E.R.C. conceived this research, designed the experiments, and wrote the manuscript. All authors reviewed and approved the manuscript.

Data Availability Statement

All data generated or analyzed during this study are included in this article and its online supplementary material. Further inquiries can be directed to the corresponding authors.

References

1 Hase K, Eckmann L, Leopard JD, Varki N, Kagnoff MF. Cell differentiation is a key determinant of cathelicidin LL-37/human cationic antimicrobial protein 18 expression by human colon epithelium. Infect Immun. 2002 Feb;70(2):953–63.
2 Zanetti M. Cathelicidins, multifunctional peptides of the innate immunity. J Leukocyte Biol. 2004 Jan;75(1):39–48.
3 Alford MA, Baquir B, Santana FL, Haney EF, Hancock REW. Cathelicidin host defense peptides and inflammatory signaling: striking a balance. Front Microbiol. 2020;11:1902.
4 Mookherjee N, Anderson MA, Haagsman HP, Davidson DJ. Antimicrobial host defence peptides: functions and clinical potential. Nat Rev Drug Discov. 2020 May;19(5):311–32.

5 Hancock REW, Haney EF, Gill EE. The immunology of host defence peptides: beyond antimicrobial activity. Nat Rev Immunol. 2016 May;16(5):321–34.
6 Scott A, Weldon S, Buchanan PJ, Schock B, Ernst RK, McAuley DF, et al. Evaluation of the ability of LL-37 to neutralise LPS in vitro and ex vivo. PLoS One. 2011;6(10):e26525.
7 Smith JJ, Travis SM, Greenberg EP, Welsh MJ. Cystic fibrosis airway epithelia fail to kill bacteria because of abnormal airway surface fluid. Cell. 1996 Apr 19;85(2):229–36.
8 Guo L, Lim KB, Poduje CM, Daniel M, Gunn JS, Hackett M, et al. Lipid A acylation and bacterial resistance against vertebrate antimicrobial peptides. Cell. 1998 Oct 16;95(2):189–98.
9 Benincasa M, Scocchi M, Pacor S, Tossi A, Nobili D, Basaglia G, et al. Fungicidal activity of five cathelicidin peptides against clinically isolated yeasts. J Antimicrob Chemother. 2006 Nov;58(5):950–9.
10 Liu YF, Luan C, Xia X, An S, Wang YZ. Antibacterial activity, cytotoxicity and mechanism of action of cathelicidin peptides against enteric pathogens in weaning piglets. Int J Pept Res Ther. 2011;17:175–84.
11 Byfield FJ, Wen Q, Leszczynska K, Kulakowska A, Namiot Z, Janmey PA, et al. Cathelicidin LL-37 peptide regulates endothelial cell stiffness and endothelial barrier permeability. Am J Physiol Cell Physiol. 2011 Jan;300(1):C105–12.
12 Schaller-Bals S, Schulze A, Bals R. Increased levels of antimicrobial peptides in tracheal aspirates of newborn infants during infection. Am J Respir Crit Care Med. 2002 Apr 1; 165(7):992–5.
13 Murakami T, Suzuki K, Niyonsaba F, Tada H, Reich J, Tamura H, et al. MrgX2mediated internalization of LL37 and degranulation of human LAD2 mast cells. Mol Med Rep. 2018 Dec;18(6):4951–9.
14 De Y, Chen Q, Schmidt AP, Anderson GM, Wang JM, Wooters J, et al. LL-37, the neutrophil granule- and epithelial cell-derived cathelicidin, utilizes formyl peptide receptor-like 1 (FPRL1) as a receptor to chemoattract human peripheral blood neutrophils, monocytes, and T cells. J Exp Med. 2000 Oct 2; 192(7):1069–74.
15 Tjabringa GS, Ninaber DK, Drijfhout JW, Rabe KF, Hiemstra PS. Human cathelicidin LL-37 is a chemoattractant for eosinophils and neutrophils that acts via formyl-peptide receptors. Int Arch Allergy Immunol. 2006; 140(2):103–12.
16 Zhang Z, Cherryholmes G, Chang F, Rose DM, Schraufstatter I, Shively JE. Evidence that cathelicidin peptide LL-37 may act as a functional ligand for CXCR2 on human neutrophils. Eur J Immunol. 2009 Nov;39(11): 3181–94.
17 Lishko VK, Moreno B, Podolnikova NP, Ugarova TP. Identification of human cathelicidin peptide ll-37 as a ligand for macrophage integrin αmβ2 (Mac-1, CD11b/CD18) that promotes phagocytosis by opsonizing bacteria. Res Rep Biochem. 2016 Jul 7;2016(6):39–55.
18 Wan M, van der Does AM, Tang X, Lindbom L, Agerberth B, Haeggstrom JZ. Antimicrobial peptide LL-37 promotes bacterial phagocytosis by human macrophages. J Leukoc Biol. 2014 Jun;95(6):971–81.
19 Kuroda K, Okumura K, Isogai H, Isogai E. The human cathelicidin antimicrobial peptide LL-37 and mimics are potential anticancer drugs. Front Oncol. 2015;5:144.
20 Tang X, Basavarajappa D, Haeggstrom JZ, Wan M. P2X7 receptor regulates internalization of antimicrobial peptide LL-37 by human macrophages that promotes intracellular pathogen clearance. J Immunol. 2015 Aug 1; 195(3):1191–201.
21 Mookherjee N, Brown KL, Bowdish DME, Doria S, Falsafi R, Hokamp K, et al. Modulation of the TLR-mediated inflammatory response by the endogenous human host defense peptide LL-37. J Immunol. 2006 Feb 15; 176(4):2455–64.
22 van Harten RM, van Woudenbergh E, van Dijk A, Haagsman HP. Cathelicidins: immunomodulatory antimicrobials. Vaccines. 2018 Sep 14;6(3):63.
23 van der Does AM, Hiemstra PS, Mookherjee N. Antimicrobial host defence peptides: immunomodulatory functions and translational prospects. Adv Exp Med Biol. 2019;1117:149–71.
24 Scheenstra MR, van Harten RM, Veldhuizen EJA, Haagsman HP, Coorens M. Cathelicidins modulate TLR-activation and inflammation. Front Immunol. 2020;11:1137.
25 Nagaoka I, Hirota S, Niyonsaba F, Hirata M, Adachi Y, Tamura H, et al. Cathelicidin family of antibacterial peptides CAP18 and CAP11 inhibit the expression of TNF-alpha by blocking the binding of LPS to CD14(+) cells. J Immunol. 2001 Sep 15;167(6):3329–38.
26 Rosenfeld Y, Papo N, Shai Y. Endotoxin (lipopolysaccharide) neutralization by innate immunity host-defense peptides. Peptide properties and plausible modes of action. J Biol Chem. 2006 Jan 20;281(3):1636–43.
27 Holani R, Babbar A, Blyth GAD, Lopes F, Jijon H, McKay DM, et al. Cathelicidin-mediated lipopolysaccharide signaling via intracellular TLR4 in colonic epithelial cells evokes CXCL8 production. Gut Microbes. 2020 Jul 13;12(1):1785802.
28 Agier J, Brzezinska-Blaszczyk E, Zelechowska P, Wiktorska M, Pietrzak J, Rozalska S. Cathelicidin LL-37 affects surface and intracellular Toll-like receptor expression in tissue mast cells. J Immunol Res. 2018;2018:7357162.
29 Aidoukovitch A, Anders E, Dahl S, Nebel D, Svensson D, Nilsson BO. The host defense peptide LL-37 is internalized by human periodontal ligament cells and prevents LPS-induced MCP-1 production. J Periodontal Res. 2019 Dec;54(6):662–70.
30 Amatngalim GD, Nijnik A, Hiemstra PS, Hancock REW. Cathelicidin peptide LL-37 modulates TREM-1 expression and inflammatory responses to microbial compounds. Inflammation. 2011 Oct;34(5):412–25.
31 Chen Y, Cai S, Qiao X, Wu M, Guo Z, Wang R, et al. As-CATH1-6, novel cathelicidins with potent antimicrobial and immunomodulatory properties from *Alligator sinensis*, play pivotal roles in host antimicrobial immune responses. Biochem J. 2017 Aug 10; 474(16):2861–85.
32 Qiao X, Yang H, Gao J, Zhang F, Chu P, Yang Y, et al. Diversity, immunoregulatory action and structure-activity relationship of green sea turtle cathelicidins. Dev Comp Immunol. 2019 Sep;98:189–204.
33 Kulkarni NN, O'Neill AM, Dokoshi T, Luo EWC, Wong GCL, Gallo RL. Sequence determinants in the cathelicidin LL-37 that promote inflammation via presentation of RNA to scavenger receptors. J Biol Chem. 2021 Jul; 297(1):100828.
34 Lande R, Gregorio J, Facchinetti V, Chatterjee B, Wang YH, Homey B, et al. Plasmacytoid dendritic cells sense self-DNA coupled with antimicrobial peptide. Nature. 2007 Oct 4; 449(7162):564–9.
35 Nizet V, Ohtake T, Lauth X, Trowbridge J, Rudisill J, Dorschner RA, et al. Innate antimicrobial peptide protects the skin from invasive bacterial infection. Nature. 2001 Nov 22; 414(6862):454–7.
36 Pinheiro da Silva F, Gallo RL, Nizet V. Differing effects of exogenous or endogenous cathelicidin on macrophage Toll-like receptor signaling. Immunol Cell Biol. 2009 Aug–Sep; 87(6):496–500.
37 Chamorro CI, Weber G, Gronberg A, Pivarcsi A, Stahle M. The human antimicrobial peptide LL-37 suppresses apoptosis in keratinocytes. J Invest Dermatol. 2009 Apr;129(4): 937–44.
38 Song D, Zong X, Zhang H, Wang T, Yi H, Luan C, et al. Antimicrobial peptide Cathelicidin-BF prevents intestinal barrier dysfunction in a mouse model of endotoxemia. Int Immunopharmacol. 2015 Mar;25(1):141–7.
39 Burns K, Clatworthy J, Martin L, Martinon F, Plumpton C, Maschera B, et al. Tollip, a new component of the IL-1RI pathway, links IRAK to the IL-1 receptor. Nat Cell Biol. 2000 Jun;2(6):346–51.
40 Diao N, Zhang Y, Chen K, Yuan R, Lee C, Geng S, et al. Deficiency in Toll-interacting protein (Tollip) skews inflamed yet incompetent innate leukocytes in vivo during DSS-induced septic colitis. Sci Rep. 2016 Oct 5;6: 34672.
41 Hou Y, Lu X, Zhang Y. IRAK inhibitor protects the intestinal tract of necrotizing enterocolitis by inhibiting the Toll-like receptor (TLR) inflammatory signaling pathway in rats. Med Sci Monit. 2018 May 22;24:3366–73.
42 Maillard MH, Bega H, Uhlig HH, Barnich N, Grandjean T, Chamaillard M, et al. Toll-interacting protein modulates colitis susceptibility in mice. Inflamm Bowel Dis. 2014 Apr;20(4): 660–70.

43 Begka C, Pattaroni C, Mooser C, Nancey S; Swiss IBD Cohort Study Group; McCoy KD, et al. Toll-interacting protein regulates immune cell infiltration and promotes colitis-associated cancer. iScience. 2020 Mar 27; 23(3):100891.
44 Inomata M, Horie T, Into T. Effect of the antimicrobial peptide LL-37 on gene expression of chemokines and 29 Toll-like receptor-associated proteins in human gingival fibroblasts under stimulation with *Porphyromonas gingivalis* lipopolysaccharide. Probiotics Antimicrob Proteins. 2020 Mar;12(1):64–72.
45 Maaser C, Housley MP, Iimura M, Smith JR, Vallance BA, Finlay BB, et al. Clearance of *Citrobacter rodentium* requires B cells but not secretory immunoglobulin A (IgA) or IgM antibodies. Infect Immun. 2004 Jun;72(6): 3315–24.
46 Moshkovskaya M, Vakhrusheva T, Rakitina D, Baykova J, Panasenko O, Basyreva L, et al. Neutrophil activation by *Escherichia coli* isolates from human intestine: effects of bacterial hydroperoxidase activity and surface hydrophobicity. FEBS Open Bio. 2020 Mar; 10(3):414–26.
47 Mullineaux-Sanders C, Sanchez-Garrido J, Hopkins EGD, Shenoy AR, Barry R, Frankel G. *Citrobacter rodentium*-host-microbiota interactions: immunity, bioenergetics and metabolism. Nat Rev Microbiol. 2019 Nov; 17(11):701–15.
48 Hing TC, Ho S, Shih DQ, Ichikawa R, Cheng M, Chen J, et al. The antimicrobial peptide cathelicidin modulates *Clostridium difficile*-associated colitis and toxin A-mediated enteritis in mice. Gut. 2013 Sep;62(9):1295–305.
49 Xu B, Wu X, Gong Y, Cao J. IL-27 induces LL-37/CRAMP expression from intestinal epithelial cells: implications for immunotherapy of *Clostridioides difficile* infection. Gut Microbes. 2021 Jan–Dec;13(1):1968258.
50 Tai EKK, Wu WKK, Wang XJ, Wong HPS, Yu L, Li ZJ, et al. Intrarectal administration of mCRAMP-encoding plasmid reverses exacerbated colitis in Cnlp(−/−) mice. Gene Ther. 2013 Feb;20(2):187–93.
51 Zheng X, Peng M, Li Y, Wang X, Lu W, Wang X, et al. Cathelicidin-related antimicrobial peptide protects against cardiac fibrosis in diabetic mice heart by regulating endothelial-mesenchymal transition. Int J Biol Sci. 2019; 15(11):2393–407.
52 Wang X, Chen L, Zhao X, Xiao L, Yi S, Kong Y, et al. A cathelicidin-related antimicrobial peptide suppresses cardiac hypertrophy induced by pressure overload by regulating IGFR1/PI3K/AKT and TLR9/AMPKα. Cell Death Dis. 2020 Feb 6;11(2):96.
53 Freitas CG, Lima SMF, Freire MS, Cantuaria APC, Junior NGO, Santos TS, et al. An immunomodulatory peptide confers protection in an experimental candidemia murine model. Antimicrob Agents Chemother. 2017; 61(8):e02518-16.
54 Fernando EH, Dicay M, Stahl M, Gordon MH, Vegso A, Baggio C, et al. A simple, cost-effective method for generating murine colonic 3D enteroids and 2D monolayers for studies of primary epithelial cell function. Am J Physiol Gastrointest Liver Physiol. 2017 Nov 1;313(5):G467–75.
55 Weischenfeldt J, Porse B. Bone marrow-derived macrophages (BMM): isolation and applications. CSH Protoc. 2008 Dec 1;2008:pdb.prot5080.
56 Bustin SA, Benes V, Garson JA, Hellemans J, Huggett J, Kubista M, et al. The MIQE guidelines: minimum information for publication of quantitative real-time PCR experiments. Clin Chem. 2009 Apr;55(4):611–22.
57 Cox J, Neuhauser N, Michalski A, Scheltema RA, Olsen JV, Mann M. Andromeda: a peptide search engine integrated into the MaxQuant environment. J Proteome Res. 2011 Apr 1;10(4):1794–805.
58 Cox J, Mann M. MaxQuant enables high peptide identification rates, individualized p.p.b.-range mass accuracies and proteome-wide protein quantification. Nat Biotechnol. 2008 Dec;26(12):1367–72.
59 Marin M, Holani R, Shah CB, Odeon A, Cobo ER. Cathelicidin modulates synthesis of Toll-like receptors (TLRs) 4 and 9 in colonic epithelium. Mol Immunol. 2017 Nov;91:249–58.
60 Marin M, Holani R, Blyth GAD, Drouin D, Odeon A, Cobo ER. Human cathelicidin improves colonic epithelial defenses against *Salmonella typhimurium* by modulating bacterial invasion, TLR4 and pro-inflammatory cytokines. Cell Tissue Res. 2019 Jun;376(3): 433–42.
61 Ren SX, Cheng ASL, To KF, Tong JHM, Li MS, Shen J, et al. Host immune defense peptide LL-37 activates caspase-independent apoptosis and suppresses colon cancer. Cancer Res. 2012 Dec 15;72(24):6512–23.
62 Zhang G, Ghosh S. Negative regulation of Toll-like receptor-mediated signaling by Tollip. J Biol Chem. 2002 Mar 1;277(9):7059–65.
63 Didierlaurent A, Brissoni B, Velin D, Aebi N, Tardivel A, Kaslin E, et al. Tollip regulates proinflammatory responses to interleukin-1 and lipopolysaccharide. Mol Cell Biol. 2006 Feb;26(3):735–42.
64 Gebert LFR, MacRae IJ. Regulation of microRNA function in animals. Nat Rev Mol Cell Biol. 2019 Jan;20(1):21–37.
65 Sugi Y, Takahashi K, Kurihara K, Nakata K, Narabayashi H, Hamamoto Y, et al. Post-transcriptional regulation of toll-interacting protein in the intestinal epithelium. PLoS One. 2016;11(10):e0164858.
66 Li T, Hu J, Li L. Characterization of Tollip protein upon lipopolysaccharide challenge. Mol Immunol. 2004 May;41(1):85–92.
67 Suzuki K, Murakami T, Kuwahara-Arai K, Tamura H, Hiramatsu K, Nagaoka I. Human anti-microbial cathelicidin peptide LL-37 suppresses the LPS-induced apoptosis of endothelial cells. Int Immunol. 2011 Mar;23(3): 185–93.
68 Nagaoka I, Tamura H, Hirata M. An antimicrobial cathelicidin peptide, human CAP18/LL-37, suppresses neutrophil apoptosis via the activation of formyl-peptide receptor-like 1 and P2X7. J Immunol. 2006 Mar 1;176(5): 3044–52.
69 Li X, Kim SE, Chen TY, Wang J, Yang X, Tabib T, et al. Toll interacting protein protects bronchial epithelial cells from bleomycin-induced apoptosis. FASEB J. 2020 Jun 28; 34(8):9884–98.
70 Kitamura S, Miyazaki Y, Shinomura Y, Kondo S, Kanayama S, Matsuzawa Y. Peroxisome proliferator-activated receptor gamma induces growth arrest and differentiation markers of human colon cancer cells. Jpn J Cancer Res. 1999 Jan;90(1):75–80.
71 Takashima T, Fujiwara Y, Higuchi K, Arakawa T, Yano Y, Hasuma T, et al. PPAR-gamma ligands inhibit growth of human esophageal adenocarcinoma cells through induction of apoptosis, cell cycle arrest and reduction of ornithine decarboxylase activity. Int J Oncol. 2001 Sep;19(3):465–71.
72 Scott MG, Davidson DJ, Gold MR, Bowdish D, Hancock REW. The human antimicrobial peptide LL-37 is a multifunctional modulator of innate immune responses. J Immunol. 2002 Oct 1;169(7):3883–91.
73 Molhoek EM, den Hertog AL, de Vries AMBC, Nazmi K, Veerman ECI, Hartgers FC, et al. Structure-function relationship of the human antimicrobial peptide LL-37 and LL-37 fragments in the modulation of TLR responses. Biol Chem. 2009 Apr;390(4):295–303.
74 Coorens M, Schneider VAF, de Groot AM, van Dijk A, Meijerink M, Wells JM, et al. Cathelicidins inhibit *Escherichia coli*-induced TLR2 and TLR4 activation in a viability-dependent manner. J Immunol. 2017 Aug 15; 199(4):1418–28.
75 Byun EB, Kim WS, Sung NY, Byun EH. Epigallocatechin-3-gallate regulates anti-Inflammatory action through 67-kDa laminin receptor-mediated Tollip signaling induction in lipopolysaccharide-stimulated human intestinal epithelial cells. Cell Physiol Biochem. 2018;46(5):2072–81.
76 Liu Y, Zhang Q, Ding Y, Li X, Zhao D, Zhao K, et al. Histone lysine methyltransferase Ezh1 promotes TLR-triggered inflammatory cytokine production by suppressing Tollip. J Immunol. 2015 Mar 15;194(6):2838–46.
77 Watts BA 3rd, Tamayo E, Sherwood ER, Good DW. Monophosphoryl lipid A induces protection against LPS in medullary thick ascending limb through induction of Tollip and negative regulation of IRAK-1. Am J Physiol Renal Physiol. 2019 Sep 1;317(3):F705–19.
78 Ren Z, Pan LL, Huang Y, Chen H, Liu Y, Liu H, et al. Gut microbiota-CRAMP axis shapes intestinal barrier function and immune responses in dietary gluten-induced enteropathy. EMBO Mol Med. 2021 Aug 9;13(8): e14059.

79 Biswas D, Ambalavanan P, Ravins M, Anand A, Sharma A, Lim KXZ, et al. LL-37-mediated activation of host receptors is critical for defense against group A streptococcal infection. Cell Rep. 2021 Mar 2;34(9):108766.
80 Tokumaru S, Sayama K, Shirakata Y, Komatsuzawa H, Ouhara K, Hanakawa Y, et al. Induction of keratinocyte migration via transactivation of the epidermal growth factor receptor by the antimicrobial peptide LL-37. J Immunol. 2005 Oct 1;175(7):4662–8.
81 Niyonsaba F, Ushio H, Nakano N, Ng W, Sayama K, Hashimoto K, et al. Antimicrobial peptides human beta-defensins stimulate epidermal keratinocyte migration, proliferation and production of proinflammatory cytokines and chemokines. J Invest Dermatol. 2007 Mar;127(3):594–604.
82 Chen X, Resh MD. Cholesterol depletion from the plasma membrane triggers ligand-independent activation of the epidermal growth factor receptor. J Biol Chem. 2002 Dec 20;277(51):49631–7.
83 Seike M, Goto A, Okano T, Bowman ED, Schetter AJ, Horikawa I, et al. MiR-21 is an EGFR-regulated anti-apoptotic factor in lung cancer in never-smokers. Proc Natl Acad Sci U S A. 2009 Jul 21;106(29):12085–90.
84 Chendrimada TP, Gregory RI, Kumaraswamy E, Norman J, Cooch N, Nishikura K, et al. TRBP recruits the Dicer complex to Ago2 for microRNA processing and gene silencing. Nature. 2005 Aug 4;436(7051):740–4.
85 Shankar S, Tien JCY, Siebenaler RF, Chugh S, Dommeti VL, Zelenka-Wang S, et al. An essential role for Argonaute 2 in EGFR-KRAS signaling in pancreatic cancer development. Nat Commun. 2020 Jun 4;11(1):2817.
86 Shen J, Xia W, Khotskaya YB, Huo L, Nakanishi K, Lim SO, et al. EGFR modulates microRNA maturation in response to hypoxia through phosphorylation of AGO2. Nature. 2013 May 16;497(7449):383–7.
87 Zhu H, Dougherty U, Robinson V, Mustafi R, Pekow J, Kupfer S, et al. EGFR signals downregulate tumor suppressors miR-143 and miR-145 in Western diet-promoted murine colon cancer: role of G1 regulators. Mol Cancer Res. 2011 Jul;9(7):960–75.
88 Fang X, Yu SX, Lu Y, Bast RC Jr, Woodgett JR, Mills GB. Phosphorylation and inactivation of glycogen synthase kinase 3 by protein kinase A. Proc Natl Acad Sci U S A. 2000 Oct 24;97(22):11960–5.
89 Varedi K SM, Ventura AC, Merajver SD, Lin XN. Multisite phosphorylation provides an effective and flexible mechanism for switch-like protein degradation. PLoS One. 2010 Dec 13;5(12):e14029.
90 Chen N, Xiao B, Wang S, Wei B. Bioinformatics analysis of microRNA linked to ubiquitin proteasome system in traumatic osteonecrosis of the femoral head. Medicine. 2020 Aug 14;99(33):e21706.
91 Chen Y, Choong LY, Lin Q, Philp R, Wong CH, Ang BK, et al. Differential expression of novel tyrosine kinase substrates during breast cancer development. Mol Cell Proteomics. 2007 Dec;6(12):2072–87.
92 Katoh Y, Imakagura H, Futatsumori M, Nakayama K. Recruitment of clathrin onto endosomes by the Tom1-Tollip complex. Biochem Biophys Res Commun. 2006 Mar 3;341(1):143–9.
93 Liu NS, Loo LS, Loh E, Seet LF, Hong W. Participation of Tom1L1 in EGF-stimulated endocytosis of EGF receptor. EMBO J. 2009 Nov 18;28(22):3485–99.
94 Hayashi M, Kuroda K, Ihara K, Iwaya T, Isogai E. Suppressive effect of an analog of the antimicrobial peptide of LL-37 on colon cancer cells via exosome-encapsulated miRNAs. Int J Mol Med. 2018 Dec;42(6):3009–16.
95 Larsen MT, Hager M, Glenthoj A, Asmar F, Clemmensen SN, Mora-Jensen H, et al. miRNA-130a regulates C/EBP-epsilon expression during granulopoiesis. Blood. 2014 Feb 13;123(7):1079–89.
96 Wang J, Cheng M, Law IKM, Ortiz C, Sun M, Koon HW. Cathelicidin suppresses colon cancer metastasis via a P2RX7-dependent mechanism. Mol Ther Oncolytics. 2019 Jan 29;12:195–203.
97 Lebeis SL, Bommarius B, Parkos CA, Sherman MA, Kalman D. TLR signaling mediated by MyD88 is required for a protective innate immune response by neutrophils to *Citrobacter rodentium*. J Immunol. 2007 Jul 1;179(1):566–77.
98 Negroni A, Cucchiara S, Stronati L. Apoptosis, necrosis, and necroptosis in the gut and intestinal homeostasis. Mediators Inflamm. 2015;2015:250762.
99 Simmons CP, Goncalves NS, Ghaem-Maghami M, Bajaj-Elliott M, Clare S, Neves B, et al. Impaired resistance and enhanced pathology during infection with a noninvasive, attaching-effacing enteric bacterial pathogen, *Citrobacter rodentium*, in mice lacking IL-12 or IFN-gamma. J Immunol. 2002 Feb 15;168(4):1804–12.
100 Li F, Wang HD, Lu DX, Wang YP, Qi RB, Fu YM, et al. Neutral sulfate berberine modulates cytokine secretion and increases survival in endotoxemic mice. Acta Pharmacol Sin. 2006 Sep;27(9):1199–205.
101 Baker J, Brown K, Rajendiran E, Yip A, DeCoffe D, Dai C, et al. Medicinal lavender modulates the enteric microbiota to protect against *Citrobacter rodentium*-induced colitis. Am J Physiol Gastrointest Liver Physiol. 2012 Oct;303(7):G825–36.
102 Eng VV, Pearson JS. In vivo studies on *Citrobacter rodentium* and host cell death pathways. Curr Opin Microbiol. 2021 Dec;64:60–7.
103 Mukherjee S, Biswas T. Activation of TOLLIP by porin prevents TLR2-associated IFN-gamma and TNF-alpha-induced apoptosis of intestinal epithelial cells. Cell Signal. 2014 Dec;26(12):2674–82.
104 Todorova T, Bock FJ, Chang P. PARP13 regulates cellular mRNA post-transcriptionally and functions as a pro-apoptotic factor by destabilizing TRAILR4 transcript. Nat Commun. 2014 Nov 10;5:5362.
105 Wang D, Wang H, Guo Y, Ning W, Katkuri S, Wahli W, et al. Crosstalk between peroxisome proliferator-activated receptor delta and VEGF stimulates cancer progression. Proc Natl Acad Sci U S A. 2006 Dec 12;103(50):19069–74.
106 Freeman AJ, Vervoort SJ, Michie J, Ramsbottom KM, Silke J, Kearney CJ, et al. HOIP limits anti-tumor immunity by protecting against combined TNF and IFN-gamma-induced apoptosis. EMBO Rep. 2021 Sep 1;22(11):e53391.
107 Koziel J, Bryzek D, Sroka A, Maresz K, Glowczyk I, Bielecka E, et al. Citrullination alters immunomodulatory function of LL-37 essential for prevention of endotoxin-induced sepsis. J Immunol. 2014 Jun 1;192(11):5363–72.